学　位　論　文

Analysis of a novel nuclear envelope protein, Nemp1, in early *Xenopus* eye development

アフリカツメガエル初期眼発生における新規核膜タンパク質 Nemp1 の解析

平成 20 年 12 月　博士（理学）申請

東京大学大学院理学系研究科

生物科学専攻

儘　田　博　志

Contents

Abstract

To clarify the molecular mechanisms of early brain development in vertebrates, I analyzed new candidate developmental regulator genes selected using systematic expression pattern screening with a *Xenopus* anterior neuroectoderm cDNA library. In this thesis, I describe the identification and characterization of a newly identified nuclear envelope localized protein, termed Nemp1 (nuclear envelope integral membrane protein 1). Nemp1 has a putative signal peptide and five transmembrane domains, but does not have any other known domains or motifs. *nemp1* is expressed in the anterior neuroectoderm at the neurula stage and in the head region, predominantly in the eyes, at later stages. Using the digitonin permeabilization-immunostaining method that I developed, Nemp1 is suggested to be localized to the inner nuclear membrane (INM) with its evolutionarily conserved C-terminal region facing the nucleoplasm. In functional analyses for Nemp1, both overexpression by mRNA injection and knockdown by antisense morpholino oligo injection in *Xenopus* embryos reduced the expression of early eye marker genes, *rax*, *tbx3,* and *pax6*, at the neurula stage, and later resulted mainly in severe eye defects at the tailbud stage. By contrast, the expression of a forebrain/midbrain marker, *otx2*, and a pan-neural marker, *sox2*, was largely unaffected in these injected embryos. In addition, analysis of Nemp1 deletion constructs showed that signal peptide and transmembrane domains are absolutely necessary for both eye-reducing activity and nuclear envelope localization, and importantly nuclear envelope-localization of the C-terminal region is necessary for Nemp1 activity. These data leads to the possibility that Nemp1 functions at the inner nuclear membrane as a complex, which requires a proper stoichiometry. I sought Nemp1-interacting proteins and show that *nemp1* is coexpressed with *baf* (barrier-to-

autointegration factor) in the eye anlagen, and that Nemp1 interacts with BAF through the BAF-binding site in the C-terminal region and this site is required for Nemp1 activity. These data suggest that Nemp1 is involved in the expression of eye marker genes by functioning at the INM at least partly through BAF. This is the first evidence for a role of a nuclear envelope protein in organ-specific gene expression during embryonic development.

Abbreviations

ANE, anterior neuroectoderm

BAF, barrier-to-autointegration factor

BBS, BAF binding site

Bt, region B and terminal region

Ct, C-terminal region

KR, lysine and arginine-rich region

NE, nuclear envelope

NLS, nuclear localization signal

NPC, nuclear pore complex

INM, inner nuclear membrane

ONM, outer nuclear membrane

SP, signal peptide

TM, transmembrane

WISH, whole mount in situ hybridization

Synonymous gene symbols and names

Official gene symbol (full name):	synonymous gene symbol
lemd3 (*LEM domain containing 3*):	*MAN1*
msi1 (*musashi homolog 1*):	*nrp1*
nr2e1 (*nuclear receptor subfamily 2, group E, member 1*):	*tll*
rax (*retina and anterior neural fold homeobox*):	*rx*, *Rx1*, *Rx2A*
six3 (*six homeobox 3*)	
six6 (*six homeobox 6*):	*optx2*
sox2 (*sex determining region Y-box 2*)	
tbx3 (*T-box 3*):	*ET*

Introduction

The molecular mechanisms of vertebrate development have been extensively studied mainly by focusing on secreted signaling molecules, intracellular signal transducers, and transcription factors. However, the molecular cascades from neural induction and early patterning to brain formation are not fully clarified. During early *Xenopus* development, the neuroectoderm is induced from the dorsal ectoderm of the gastrula embryo by signals from the Spemann organizer (Fig. 1) (De Robertis et al., 2000; Niehrs, 2004). The neuroectoderm then acquires regional specificity along the dorsoventral and anteroposterior axes. The early neural patterning is brought about by the expression of various region-specific genes for the presumptive midbrain–hindbrain boundary region (Shinga et al., 2001; Takada et al., 2005), the neural crest (Steventon et al., 2005), and the eye field (Bailey et al., 2004; Esteve and Bovolenta, 2006; Lupo et al., 2000), among other regions. However, the gene regulatory mechanisms underlying those region-specific expressions have not been fully elucidated. Recently, nuclear membrane proteins have been shown to play a role in signal transduction and gene regulation (Gruenbaum et al., 2005), as exemplified by *Xenopus* MAN1 (Osada et al., 2003). This thesis describes a novel nuclear membrane protein and its involvement in gene regulation for early *Xenopus* eye development.

The nuclear envelope (NE) consists of the outer (ONM) and inner (INM) nuclear membranes, nuclear pore complexes (NPCs), and nuclear lamina (Fig. 2). The ONM is directly continuous with the endoplasmic reticulum. ONM proteins, Nesprin-1, Nesprin-2 and Nesprin-3, connect to the cytoskeletal system to maintain to the appropriate position of the nucleus in the cell (Gruenbaum et al., 2005; Wilhelmsen et al., 2005; Zhang et al.,

2002). The INM contains a distinctive set of integral membrane proteins, such as LAP2, MAN1, and Emerin, which interact with the nuclear lamina, a meshwork of intermediate filament proteins that underlies the INM (Burke and Stewart, 2002). These proteins play an essential role in maintaining the structural integrity of the NE (Gruenbaum et al., 2005; Hutchison, 2002). In addition, LAP2, MAN1, and Emerin interact with barrier-to-autointegration factor (BAF) (Furukawa, 1999; Lee et al., 2001; Mansharamani and Wilson, 2005; Shumaker et al., 2001), which binds to DNA as a homodimer to form a bridge between these proteins and DNA, and is thought to be involved in chromatin decondensation and nuclear assembly (Cai et al., 1998; Margalit et al., 2007; Segura-Totten et al., 2002). Although genes for NE proteins are though to be nearly ubiquitously expressed in many types of cells, defects in NE proteins lead to a group of human diseases, known as 'laminopathies' including cardiac and skeletal myopathies and peripheral neuropathy (Burke and Stewart, 2002), implying the role of NE proteins in tissue-specific functions. For further analysis of NE, novel NE proteins have been identified by proteomic analysis (Dreger et al., 2001; Schirmer et al., 2003), but their cellular and developmental functions have not been elucidated. In this situation, it is important that Osada *et al.* in our lab have shown that the INM protein MAN1 acts as a Smad-interacting protein to antagonize BMP signaling during early *Xenopus* development (Osada et al., 2003) and to antagonize TGF-β signaling to regulate vascular remodeling in mice (Ishimura et al., 2006). Subsequently, Emerin has been shown to attenuate Wnt signaling by exporting β-catenin from the nucleus (Markiewicz et al., 2006). Thus, knowledge of the developmental roles of NE proteins is being accumulated, but identification and functional analysis of a novel INM protein are necessary for further understanding of their developmental roles.

Fate map and gene expression studies of vertebrate eye development have shown that the presumptive eye territories originate from a single bilaterally expanded field positioned within the anterior neuroectoderm (ANE) demarcated by *otx2* expression (Eagleson et al., 1995; Inoue et al., 2000; Li et al., 1997; Varga et al., 1999). To date, several transcription factors have been suggested as being involved in eye development. These transcription factors include *rax* (the same as *rx*, representing the alloalleles *Rx1* and *Rx2A*), *pax6*, and *six3* (Andreazzoli et al., 1999; Chow et al., 1999; Chuang and Raymond, 2001; Loosli et al., 1999; Mathers et al., 1997; Oliver et al., 1996). Gain of function analyses have shown that overexpression of *rax*, *pax6*, *six3* and *six6* (the same as *optx2*) can expand or induce eye tissues in the CNS of vertebrates (Andreazzoli et al., 1999; Bernier et al., 2000; Chow et al., 1999; Chuang and Raymond, 2001; Loosli et al., 1999; Mathers et al., 1997; Oliver et al., 1996; Zuber et al., 1999), but only in the region defined by *otx2* expression (Chuang and Raymond, 2002), suggesting that the Otx2-expressing region acquire the competency to form the eye. In *Xenopus*, a gene cascade of transcription factors from *otx2* and *tbx3* (the same as *ET*) through *rax* to *pax6*, and a gene network containing of *pax6*, *six3*, *lhx2*, *tll*, and *six6*, have been proposed for eye field specification (Fig. 3) (Zuber et al., 2003). Genetic analyses in the human and mouse have also shown the importance of *rax*, *pax6*, *six3*, *lhx*2, *tll*, and *six6* genes in eye development (Hill et al., 1991; Lagutin et al., 2003; Li et al., 2002; Mathers et al., 1997; Porter et al., 1997; Tucker et al., 2001; Yu et al., 2000). Although eye development has thus been extensively studied, the mechanisms of gene regulation of these transcription factors have not been fully investigated.

To clarify the molecular mechanisms of early neural patterning and brain development in vertebrates, our lab including me has previously performed a systematic expression pattern screening with a *Xenopus* ANE cDNA library and obtained new candidate genes for

developmental regulators (Fig. 4) (Takahashi et al., 2005). I found that one of these candidates encodes an NE protein, and named it Nemp1 for nuclear envelope integral membrane protein 1. In this thesis, I describe the identification of *nemp1* and the characterization of molecular functions and developmental roles of Nemp1 in the *Xenopus* embryo. *nemp1* is expressed in the ANE and is involved mainly in eye development from the late gastrula to the neurula stage. The functional and biochemical data suggest that the involvement of Nemp1 protein in gene regulation for eye development through binding to BAF, shedding light on both the molecular mechanisms of early eye development and the role of an INM protein in gene regulation.

Results

Isolation of a nuclear envelope protein, Nemp1

To obtain novel neural genes, Takahashi *et al.* have previously carried out systematic screening of an ANE cDNA library, isolated 1706 expression sequence tags (ESTs), and analyzed the expression patterns of 806 candidate genes by whole mount *in situ* hybridization (WISH). As a result, they selected 22 genes with unique expression patterns (Fig. 4) (Takahashi et al., 2005). In this study, of these selected 22 genes, I have determined the entire coding sequences of 7 possible novel genes, N17D12 (*nemp1a*), N20H12, N21E5, N23G4, N27F9, N31A5, and N32C3, by comparing with other orthologous genes which were obtained by similarity searches against ESTs databases of various organisms. Fig. 5 shows the entire amino acid sequences of these seven genes in comparison with their orthologous ones. N23G4 turned out to be the mitochondrial *glutaredoxin* (*Grx*) gene. N27F9 was recently identified as the *programmed cell death 10* (*PDCD10*) genes (Bergametti et al., 2005).

To gain insight into their molecular nature, I next examined the subcellular localization of their products using C-terminally Myc-tagged constructs (Fig. 6). COS7 cells were transfected with expression constructs, and analyzed using a confocal microscope after staining the nucleus with SytoxGreen. I found that N17D12 (Nemp1) was localized at the periphery of DNA, implying the localization at the NE. Localization of other genes was the cytoplasm (N20H12 and N27F9), the entire region (N21E5 and N31A5), possibly mitochondria (N23G4), and the nucleus (N32C3). The NE localization of N17D12 (Nemp1) was assessed by comparing with that of the INM protein MAN1. As shown in

Figs. 6 and 8A, Nemp1 was reproducibly localized around nuclear DNA, and this localization pattern was very similar to that of MAN1, suggesting that Nemp1 is a novel NE-localized protein. Therefore, I named this N17D12 gene *nemp1* (for nuclear envelope integral membrane protein 1), and focused on it for further analysis.

Computational analyses of the Nemp1 amino acid (aa) sequence predicted a signal peptide (SP; aa 1–34) and five transmembrane domains (TMs; aa 148–170, 175–197, 207–226, 239–261, and 276–298, according to a Kyte–Doolittle hydropathy plot) (Figs. 7A, 7B), but no known domains or motifs. In addition, I noticed potential nuclear localization signals (NLSs; K-K/R-X-K/R) in a lysine and arginine-rich sequence (RKIKRKRAK; aa 317–325), termed KR, which contains two potential overlapping NLSs, KRKR and KRAK. In addition, I found a sequence (SRIQSPKR; aa 368–375) similar to a consensus BAF binding site (BBS; S-R/K-V-X-X-X-X-R/K) (see Fig. 16A) (Mansharamani and Wilson, 2005). To examine the evolutionary conservation of Nemp1, blastp and psi-blast searches were carried out, and these showed that Nemp1 has high identities to human KIAA0286 (61.7%) and to other uncharacterized predicted proteins from fish to *Caenorhabditis elegans*, and has two evolutionarily conserved regions, named Region A and Region B, which show more than 40% identity between human and *C. elegans* (Fig. 7C). Because *Xenopus laevis* is allotetraploid, I obtained alloalleles, *nemp1a* and *nemp1b*. The amino acid sequence identity between Nemp1a and Nemp11b is 88.0% in the entire region, and 91.1% and 88.6% in Regions A and B, respectively.

INM localization of Nemp1

The NE localization of Nemp1 is shown in Fig. 8A. COS7 cells were transfected with expression constructs for Nemp1-Myc or the INM protein MAN1-Myc, and analyzed using a confocal microscope after staining the nucleus with SytoxGreen. Nemp1-Myc (red) was detected around nuclear DNA (green), which is similar to that of MAN1-Myc, suggesting that Nemp1 is an NE protein. I next examined whether Nemp1 is localized to the INM or ONM, and whether or not the C-terminus of Nemp1 is oriented to the nucleoplasm.

In order to distinguish protein localization in the INM from the ONM, I utilized digitonin in comparison with Triton X-100. Triton X-100 permeabilizes all membrane structures of the cell, whereas digitonin is known to selectively permeabilize the plasma membrane and leaves the NE intact. However, it has not been tested whether digitonin differentially permeabilizes the ONM and the INM. To examine this, I constructed a molecular probe, MAN1-HAi, which is supposed to localize its HA tags in the lumen (see Fig. 8D). In addition, I utilized Nemp1-Bt-Myc (Bt-Myc; the Nemp1 C-terminus containing aa 326–434), which was found to be ubiquitously distributed in the cell (see Figs. 13A and 14M), to identify cotransfected cells and also to assess the integrity of the NE (see Fig. 8D). COS7 cells were cotransfected with MAN1-HAi and Bt-Myc, and permeabilized with digitonin or Triton X-100 before immunostaining. As shown in Fig. 8B (rightmost panels), Triton X-100 treatment showed the ubiquitous distribution of Bt-Myc in the cell and the NE localization of MAN1-HAi. By contrast, in digitonin-treated cells, I observed differential staining patterns of Bt-Myc and MAN1-HAi, which were categorized into four types, 1A, 1B, 2A, and 2B, by combinations of cytoplasmic (type 1) or ubiquitous (type 2) staining of Bt-Myc, and partial (type A) or complete (type B) NE staining of MAN1-HAi (Fig. 8B). In digitonin treatment, type 1 (that is, type 1A plus 1B)

was the majority as expected, because the NE is not supposed to be permeabilized by digitonin (Fig. 8B; bar graph). In type 1 cells, I observed both types A and B, and importantly type 1B increased as treatment time of digitonin was prolonged (Fig. 8B; bar graph). This data indicates that digitonin selectively and gradually permeabilizes the ONM compared to the INM (see Fig. 8D; upper drawing). Even with this selectivity, when digitonin treatment was extended to 25 min, almost all cells showed type 2B, indicating that long treatment with digitonin can permeabilize both the ONM and the INM. In addition, even in short digitonin treatment, about one fifth were observed to be type 2 cells, maybe due to undesired breakage of the NE. Therefore, I adopted 3 min digitonin treatment and focused on type 1 cells in subsequent experiments.

To further confirm digitonin selectivity, I constructed C-terminally and N-terminally tagged Emerin, named Emerin-HAc and HAn-Emerin, respectively. Emerin has a single transmembrane domain and orients its C terminus to the lumen and its N terminus to the nucleoplasm (Bengtsson and Wilson, 2004) (see Fig. 8D). As shown in Fig. 8C, type 1 cells showed NE staining of Emerin-HAc, but not that of HAn-Emerin (panels a and c), whereas Trion X-100 treatment showed NE staining of both Emerin constructs and ubiquitous staining of Bt-Myc (panels b and e). There is a possibility that the N-terminal HA tags of HAn-Emerin might be masked with some protein, which could be removed by treatment with Triton X-100 but not with digitonin. However, this possibility is less likely because digitonin-treated type 2 cells, whose nuclei appeared to be perforated, showed NE staining of HAn-Emerin, indicating that its HA tags are accessible to antibodies without Triton X-100 treatment (panel d). These data suggest that digitonin can selectively permeabilize the ONM and leave the INM intact in order to specifically detect an epitope in the lumen and not to detect it in the nucleoplasm by immunostaining

(Fig. 8D).

Using the condition described above, orientation of the C-terminus of Nemp1 in the NE was examined by the two sets of experiments. In the first set of experiment, Nemp1-HA was coexpressed with Bt-Myc. Digitonin treatment showed that, although some weak staining of Nemp1-HA was detected in the cytoplasm, NE staining of Nemp1-HA was not detected in type 1 cells (Fig. 8E; panel a). Coexpression of Nemp1-HA and Bt-Myc was confirmed using Triton X-100 treatment (panel b). This data suggests that the C-terminus of Nemp1 faces the nucleoplasm, but not the lumen (Fig. 8D). To further confirm this, in the second set of experiment, Nemp1-Myc was coexpressed with Emerin-HAc or HAn-Emerin. When coexpressed with Emerin-HAc (lumen), Nemp1-Myc was not detected at the NE in Emerin-HAc-stained cells with digitonin treatment, whereas both were stained at the NE with Triton X-100 (panels c and d). By contrast, when coexpressed with HAn-Emerin (nucleoplasm), neither Nemp1-Myc nor HAn-Emerin was stained at the NE with digitonin treatment, whereas both were stained with Triton X-100 treatment (panels e and f). Thus, these data suggest that the C-terminus of Nemp1 faces the nucleoplasm as does the N-terminus of Emerin and therefore it is most likely that Nemp1 is localized in the INM.

Developmental expression profiles of nemp1 and baf

Developmental expression of *nemp1* in *Xenopus* embryos was analyzed by RT-PCR using RNA isolated from *Xenopus* embryos at various stages, by Northern blot, and by WISH. RT-PCR detected *nemp1* expression at all stages examined, including before and

after the midblastula transition (stage 8), indicating that this gene is expressed both maternally and zygotically (Fig. 9A). Northern blot analysis indicated that the Nemp1 transcript is 2.1 kb long (data not shown).

I examined spatial developmental expression patterns of *nemp1* in comparison with those of *baf* using WISH (Fig. 9B–D). At the early gastrula stage, *nemp1* was expressed mainly in the entire animal hemisphere (Fig. 9Ba,b). During neurulation, its expression became restricted to the ANE (Fig. 9Bc–f). At the tailbud stage, *nemp1* was expressed in various anterior regions including the anterior central nervous system (CNS), otic vesicles, and branchial arches (Fig. 9Bg). These expression patterns of *nemp1* were very similar to those of *baf* (Fig. 9C). Section examination showed that *nemp1* and *baf* are coexpressed in the diencephalon and optic vesicles (Fig. 9D). These data open the possibility that Nemp1 functionally relates to BAF as examined below.

Both overexpression and knockdown of Nemp1 lead to eye defects

To examine the function of Nemp1 during *Xenopus* development, *nemp1* mRNA was injected into the right dorsal blastomere at the four-cell stage to overexpress it in the ANE region. I found that overexpression of wild-type (WT) Nemp1 mainly caused eye defects, which were categorized into three types: no eye, trace eye, and small eye (Fig. 10A). In contrast, when Nemp1 was overexpressed in the ventral marginal zone, no phenotype was detected (data not shown), suggesting no cytotoxic effects of Nemp1. Because eye-reducing activities of Nemp1a and Nemp1b were basically indistinguishable (see Fig. 13B), I used mainly Nemp1a in subsequent experiments, unless otherwise mentioned.

To seek the primary cause of eye defects by Nemp1, I next examined the expression of early genes for eye development, *rax* (Mathers et al., 1997), *tbx3* (He et al., 1999; Li et al., 1997; Takabatake et al., 2000), and *pax6* (Hirsch and Harris, 1997), in Nemp1-overexpressing embryos by WISH. Figure 10B shows that Nemp1 overexpression reduces the expression of *rax*, *tbx3*, and *pax6* at the neurula stage in more than 80% of injected embryos. However, the expression of neural markers, *otx2* (forebrain/midbrain) (Pannese et al., 1995), *sox2* (pan-neural) (Mizuseki et al., 1998), and *nrp1* (pan-neural) (Knecht et al., 1995), was largely unchanged (Fig. 10B), which was similar to a negative control for which *globin* mRNA was injected. Because the early eye genes examined above are reportedly downstream of *otx2* in the gene cascade (Danno et al., 2008; Zuber et al., 1999), our data suggest that overexpression of Nemp1 specifically inhibits the gene cascade of eye development downstream of *otx2* and upstream of *rax*, *tbx3*, and *pax6*, leading to eye defects at the tailbud stage.

To analyze the necessity of *nemp1* in early embryogenesis, I knocked down Nemp1 activity by injecting a mixture (designated as MOab) of two antisense morpholino oligos, *nemp1a*-MO and *nemp1b*-MO, which are complementary to the sequence encompassing the exon 1–intron 1 boundary of *nemp1a* and *nemp1b*, respectively (Fig. 11A). As a control, I injected a five-base-mismatched morpholino oligo (5mmMO). I first confirmed the effectiveness of MOab by RT-PCR to detect unspliced RNAs containing the targeted exon 1–intron 1 splice junction. As shown in Fig. 11A, a 0.1 kb PCR band from spliced transcripts decreased in a dose-dependent manner, and in turn, a 2.1 kb band from unspliced transcripts increased in MOab-injected embryos. In contrast, these changes were not detected in 5mmMO-injected embryos, suggesting that MOab specifically inhibit Nemp1 activity through blocking proper splicing of *nemp1* pre-mRNA.

To examine the effects of MOab on early *Xenopus* embryogenesis, MOab was injected into the right side of embryos and compared with the uninjected left side. MOab-injected embryos (*nemp1* morphants) gastrulated almost normally, like the uninjected and 5mmMO-injected embryos. However, the effects of MOab became evident at later stages. The right eye was absent or poorly formed in *nemp1* morphants (93%, n = 61, three experiments; Fig. 11Ba) but not in 5mmMO morphants (0%, n = 50, three experiments; Fig. 11Bb). Curiously, this morphant phenotype is very similar to that of *nemp1* mRNA-injected embryos. The eye-less phenotype induced by MOab was completely or partially rescued by coinjection with *nemp1* mRNA (11% and 55%, respectively, n = 62, three experiments; Fig. 11Bc), suggesting that MOab specifically knockdown the level of the endogenous Nemp1 protein.

I next examined gene expression in *nemp1* morphants. As shown in Fig. 11C, the expression of early eye genes, *rax*, *tbx3*, *pax6,* and *six3* was reduced severely, whereas the expression of *otx2* and *sox2* was almost unaffected. These data suggest that Nemp1 is necessary for the expression of early eye maker genes. Furthermore, the similarity between the phenotypes of morphants and Nemp1-overexpressed embryos (Figs. 11 and 12) suggests that a proper expression level of Nemp1 is likely to be important for the expression of *rax*, *tbx3,* and *pax6* (see Discussion).

I have also performed rescue experiments with *pax6* and *rax* mRNA (Fig. 12). I observed that the reduction of *rax* expression by MOab was scarcely rescued by coinjection with *pax6* mRNA, but appeared to be rescued a little bit by *rax* mRNA. However, because the rescue activity of Rax seems to be weak, it may that the phenotype of Nemp1 morphants in rescued by Rax.

Activities of Nemp1-deletion constructs and their NE localization

Based on the eye defect phenotypes by overexpression of Nemp1, I examined which domains of Nemp1a are required for the eye-reducing activity, using various deletion constructs (Fig. 13A,B). Activity of ΔN is largely unchanged compared to that of WT Nemp1, whereas those of ΔA and ΔBt were decreased in this order. Interestingly, deletion of KR completely abolished the eye-reducing activity of Nemp1. In addition, deletion of the potential BBS reduced activity, implying that BAF is involved in eye defects by Nemp1 (see below). Because ΔN and ΔA have the different number of TMs, I further examined the significance of the number of TMs using constructs 3TMs and 4TMs, in which two and one TM, respectively, was deleted from WT. However, the odd (WT and 3TMs) or even (ΔN, ΔA and 4TMs) number of TMs did not appear to correlate with their activities (see Discussion). Other deletion constructs had a little or almost no activity.

The activities of deletion constructs were further analyzed for *rax* expression. As expected, ΔSP, ΔKR, SPNA, SP+TMs, ΔTMs, and SP+A did not affect *rax* expression and ΔBt weakly reduced it (Fig. 13C). Whereas ΔN and ΔA still had activity to reduce *rax* expression but were weaker than in WT. These data are roughly consistent with those for eye defects (Fig. 13B). These data suggest that eye defect phenotypes caused by Nemp1 occurs at least partly through the reduction of *rax* expression.

I next examined whether or not loss of activity is associated with loss of NE localization in Nemp1 deletion constructs using C-terminally Myc-tagged constructs of Nemp1a (Fig. 14). Similar to Nemp1b (Fig. 14A), ΔN, ΔA, ΔBt, SPNA, SP+TMs, SP+A, and ΔKR localized at the NE (Fig. 14B–H), whereas ΔSP appeared to associate with

membrane structures but did not properly localize at the NE (Fig. 14I). In contrast, ΔTMs and SP+Bt localized in the cytoplasm (Fig. 14J,K). These data indicate that the signal peptide (SP) and transmembrane domains (TMs) are necessary and, moreover, that the SP and some of TMs are sufficient for the localization to the NE. Interestingly, Ct localized inside the nucleus (Fig. 14L), whereas Bt, in which the KR sequence containing potential NLSs was deleted from Ct, was distributed ubiquitously within the cell (Fig. 14M; see also Fig. 8). Because molecules smaller than 20–40 kDa in size transit through the nuclear pore in a diffusion-controlled manner (Tran and Wente, 2006), Bt-Myc of 2,471.8 Da is expected to transit freely through the nuclear pore. As expected, KR-Myc, in which KR was attached to five Myc tags, was localized to the nucleus (Fig. 14N). These data suggest that the Nemp1 Ct region facing the nucleoplasm is required for its function in eye development and that this domain needs to be tethered to the INM for function (Fig. 17). This is in a good agreement with the possibility that Nemp1 forms a complex on the INM, as suggested from the similarity of phenotypes from overexpression and knockdown of Nemp1 as described above.

Interactions of Nemp1 and BAF

I hypothesized that Nemp1 may interact with one or more nuclear proteins either on the INM or associated with the nuclear periphery. I focused on BAF for the following reasons: (i) BAF is a nuclear protein and known to bind to several INM proteins (Burke and Stewart, 2002; Gruenbaum et al., 2005) and eye-specific transcription factors (Crx, Otx2, and Pax6) (Wang et al., 2002); (ii) *baf* and *nemp1* genes show expression in similar

regions of the embryo (Fig. 9); and Nemp1 has a possible BBS (Figs. 7A and 16A). I thus examined interactions between Nemp1 and BAF by GST pull-down assay using GST-Bt and GST-BtΔBBS as well as GST-MAN1-Ct as a positive control (Mansharamani and Wilson, 2005; Osada et al., 2003) and GST alone as a negative control. As shown in Fig. 16B, GST-MAN1-Ct and GST-Bt retained FLAG-BAF from embryo lysates more so than did GST-BtΔBBS and GST, suggesting that the Bt region of Nemp1 binds to BAF through the potential BBS.

To assess interactions between Nemp1 and BAF in the nucleus, FLAG-BAF was expressed with or without Nemp1-HA in COS7 cells or *Xenopus* embryos. As shown in Fig. 16C and 16D, FLAG-BAF alone was localized in the nucleus with almost uniform distribution. In contrast, when coexpressed with Nemp1-HA, FLAG-BAF was accumulated at the nuclear periphery and colocalized with Nemp1 present at the NE in COS7 cells and *Xenopus* embryos (Fig. 16C,D). Notably, this peripheral localization of FLAG-BAF was not seen when coexpressed with ΔBt-HA or ΔBBS-HA (Fig. 16C). These data suggest that the Bt region of Nemp1 interacts with BAF and requires the BBS in order to do so.

To examine the requirement of the BBS for Nemp1 functions, I performed rescue experiments of *nemp1* morphants with Nemp1-BBS mutants. As shown in Fig. 16E, reduction of *rax* expression by MOab was completely (33%) or partially (29%) rescued by coinjection with *nemp1* mRNA, but much less efficiently by ΔBt (5% or 14%, respectively) and ΔBBS mRNA (6% or 15%, respectively). This data suggests that the BBS of Nemp1 is important for eye development, and leads to the possibility that Nemp1 functionally interacts with BAF through the BBS.

Discussion

In this study, I screened possible novel genes using public EST databases and by analyzing subcellular localization using COS cells, and successfully identified an uncharacterized NE protein, named Nemp1. I have shown that: (1) digitonin selectively permeabilizes the ONM compared to the INM, enabling us to discriminate the orientation of an epitope tag in the nucleoplasm from that in the lumen of the NE, (2) Nemp1 is a novel INM-localized protein and *nemp1* is expressed in the presumptive head region including the eye field; (3) both overexpression and knockdown of Nemp1 specifically reduce the expression of *rax*, *tbx3,* and *pax6* but not that of *otx2* or *sox2*, and cause eye defects; (4) multiple regions including Region A, Region B, KR, and the BBS are necessary for eye-reducing activity of Nemp1; (5) together the signal peptide (SP) and transmembrane domains (TMs) are necessary and sufficient for Nemp1 to localize at the NE; (6) NE localization of Nemp1 is necessary for its activity; and (7) the BBS is required for Nemp1 to bind BAF and to function in *rax* expression. Taken together, these data suggest that Nemp1 is mainly involved in eye development at the early neurula stage and that it functions at the INM to regulate the gene cascade downstream of *otx2* and upstream of *rax*, *tbx3,* and *pax6*, as discussed below.

Selective permeabilization of the ONM with digitonin treatment

To understand the function of NE proteins, it is necessary to determine their localization and orientation at the NE. I have shown that digitonin selectively

permeabilizes the ONM through immunostaining of cells coexpressing MAN1-HAi, Emerin-HAc, or HAn-Emerin with Bt-Myc (Figs. 8B-D). The reason why I used MAN1 and Emerin as molecular probes is that both are well characterized INM proteins and their orientations have been determined (Lin et al., 2000; Ostlund et al., 1999; Tsuchiya et al., 1999; Wu et al., 2002). It is also reported that Emerin and MAN1 enter the nucleus by diffusion and are retained at the INM through the interaction of the N-terminal region of Emerin and MAN1 (Ostlund et al., 1999; Wu et al., 2002). This means that most of NE-retained Emerin or MAN1 molecules localize at the INM and orient their C-terminus or inter-region between the two TMs, respectively, toward the lumen (Fig. 8D). Using these constructs, I found that that digitonin gradually permeabilizes the ONM as treatment time increased (Fig. 8B). I noticed that the NE in many of type 1 cells is partially stained (type A) when digitonin treatment time is short, indicating that digitonin locally permeabilizes a part of the ONM, but the other region is intact. This implies that digitonin-treated cells have 'partially' functional nuclei, which have been used for nuclear transport assays as the standard method (Adam et al., 1990) and also for immunostaining of membrane-anchored proteins to discriminate the nucleoplasmic face from the cytoplasmic face at the NE (Brachner et al., 2005; Hieda et al., 2008; Soullam and Worman, 1993), but not from the lumenal face. Thus, this is the first evidence that digitonin selectively permeabilize the ONM compared to the INM.

In the digitonin permeabilization-immunostaining method that I develop, nucleoplasmically localized epitope tags are identified as negative immunostaining, whereas the existence of these tags facing the nucleoplasm is confirmed by immunostaining using Triton X-100 treatment. However, there is the possibility that Myc or HA tags are masked in the nucleus, which are unmasked with Triton X-100 treatment.

For example, Nup96 and Nup98 exist on both sides of the nuclear pore, but cytoplasmically localized Nup96 and Nup98 proteins are immunostained only with Trion X-100 but not with digitonin treatment, indicating that these proteins are likely masked by additional proteins present on the cytoplasmic face (Griffis et al., 2003). In this case, anti-Nup96 and Nup98 antibodies were used to detect the endogenous proteins, which form complexes in vivo. By contrast, I used overexpressed exogenous proteins, which contain fairly long tandemly repeated epitope tags, five-repeat Myc (101 residues) and four-repeat HA (68 residues for HAn and 73 residues for HAc). Therefore, it is unlikely that four to five-repeated Myc or HA epitopes of overexpressed exogenous proteins are all masked with endogenous proteins. This expectation is also supported by the following result (see also Supplementary Figure). I observed that a small population (12%) of cells treated with digitonin show NE staining of HAn-Emerin (nucleoplasm), but this staining was only seen in the cells that Bt was ubiquitously stained (type 2; see Fig. 8Cd). This means that, once the nucleus is perforated, though it is not known how this happens, the inside of nucleus is accessible to antibodies, which then react with Bt-Myc and HAc-Emerin. That is, the epitope tags of HAc-Emerin as well as Bt-Myc are not all masked in the nuclei without Triton X-100 treatment. Thus, the digitonin permeabilization-immunostaining method using tagged proteins is a convenient and useful technique to examine the orientation of NE proteins.

INM localization and activity of Nemp1

By using the digitonin permeabilization-immunostaining method, I have shown that the

Nemp1 C-terminus faces the nucleoplasm in a manner similar to HAn-Emerin (Fig. 8D). Therefore, it is very likely that Nemp1 is an INM protein and interacts with some nuclear proteins through the Ct region. Importantly, soluble types of Nemp1 constructs, Ct and Bt, localize in the nucleus (Fig. 14), but do not have eye-reducing activity (Fig. 13), suggesting that Nemp1 requires INM localization for functioning. The orientation of the C-terminus to the nucleoplasm did not appear to depend on the number of TMs, because the odd (WT and 3TMs) and even (ΔN, ΔA and 4TMs) number of TMs did not correlate with their activities (Fig. 13). It is therefore possible to speculate that the Ct region may contribute to determine its orientation to the nucleoplasm. Regarding the role of Ct, it should also be noted that both overexpression and knockdown of Nemp1 lead to the same eye defects (Figs 10 and 11), leading to the idea that Nemp1 might well form a complex with one or more nuclear proteins and must do so with proper stoichiometry at the INM through Ct, and therefore a proper level of Nemp1 expression is critical for the proper function in the eye field. I assume that Nemp1 interacts with multiple proteins to form a functional complex.

One of such proteins is suggested to be BAF, because I have shown that the Bt region interacts with BAF through the BBS (Fig. 16), and because the BBS of Nemp1 is perfectly conserved from human to zebrafish and is similar to the those found in MAN1, Crx, and histone H1.1 (Mansharamani and Wilson, 2005; Montes de Oca et al., 2005) (Fig. 16A). BAF is known to form a homodimer and to bind the LEM domain that is possessed in common by LAP2, Emerin, and MAN1 (Cai et al., 2007; Cai et al., 1998; Mansharamani and Wilson, 2005; Margalit et al., 2007; Segura-Totten et al., 2002). The binding surface on the BAF dimer for the LEM domain resides in a cleft between the two BAF subunits, whereas the binding surface for the BBS resides in each BAF subunit near its DNA binding

surface. Therefore, I speculate that Nemp1 might interact via a BAF homodimer with LEM-domain proteins and BBS-containing proteins.

The N-terminal part of Ct has KR, which is also important for Nemp1 activity (Fig. 13). KR is rich in lysine and arginine, and includes canonical NLS sequences (Figs. 7A and 14N), suggesting the possibility that KR interacts with DNA or importin α/α-karyopherin (Lange et al., 2007) and this interaction may be involved in INM localization of Nemp1 as recently shown in yeast (King et al., 2006) or may have some roles in Nemp1 functions at the INM. It was reported that, in systematic analysis for two-hybrid-based protein-interaction maps of the fly and nematode proteome, *Drosophila* and *C. elegans* orthologs of Nemp1 possibly interact with several transcription factors with unknown functions and Ran, a small GTPase with a role in nuclear transport (Giot et al., 2003; Li et al., 2004). Nemp1 may interact with those proteins at the INM. Thus, Nemp1 can form a complex with BAF, importin α, and Ran as well as with some other proteins, which may interact with region B as well as the evolutionarily conserved region A in the TM region, and indirectly with certain transcription factors and LEM-domain-containing INM proteins through a BAF homodimer.

It will be interesting to analyze whether Nemp1 binds nuclear factor NPC proteins or NE proteins, and how Nemp1 functions as a modulator in eye development. Therefore, it is important to search Nemp1-interacting proteins in vertebrates as a next step to elucidate the mechanism responsible for the role of NE protein in development (Fig. 17).

Role of Nemp1 in eye development

Our results suggest that Nemp1 acts downstream of *otx2* and upstream of *tbx3*, *rax,* and *pax6* in eye development in the ANE (Figs 10. 11, and 18). In *Xenopus*, a gene cascade of transcription factors from *otx2* and *tbx3* through *rax* to *pax6* has been proposed for eye field specification (Zuber et al., 2003). Recently, it was reported that Otx2 can activate the *rax* gene in animal caps and in reporter assays using cultured cells (Danno et al., 2008). Based on this gene cascade, Nemp1 may act on Otx2 for *rax* expression. Based on this cascade, Nemp1 may act on *otx2* for *rax* expression. It should be noted that BAF reportedly binds to the transcription factors, Otx2, Pax6, and Crx, all of which are involved in early eye development and retina differentiation, and that, in a reporter assay using cultured cells, BAF represses the function of Crx, a paralog of Otx2, by binding to the helix 3 in its homeodomain (Wang et al., 2002). Therefore, it could be thought that BAF-associated INM proteins have a role in eye development, but no experimental evidence has been reported. My data in this paper provide the first evidence for the connection between the BAF-associated INM protein Nemp1 and eye-field specific gene expression in vivo (Figs. 10, 11, 13, 16, and 18). The precise mechanism of how Nemp1 regulates the *rax* gene is not known yet, but it is possible to speculate that Nemp1 binds to BAF at the INM as a complex to activate the Otx2 protein, either directly or indirectly, for upregulation of the *rax* gene. However, because no loss-of-function study has been performed for *tbx3*, it is not known whether *tbx3* is required for *rax* expression. Therefore, it is possible that Nemp1 regulates all or some of *rax*, *tbx3,* and *pax6* genes (Fig. 18).

Disruption of genes for NE proteins such as Emerin and MAN1 leads to defects in chromosome segregation in *C. elegans* (Liu et al., 2003; Liu et al., 2000) and apoptotic cell death in mice (Ishimura et al., 2006) because of improper formation or loss of integrity of

the NE. In the case of Nemp1-knockdown in *Xenopus* embryos, there are no gross changes of the expression of *sox2* and *nrp1* as well as *otx2* expression, implying that no massive cell death occurs in the injected regions. Thus, Nemp1 may have a role in gene regulation rather than in a maintaining the integrity of the NE. It will be interesting to examine whether Nemp1 influences gene regulation in other tissues or organs, because Nem1p is expressed in various regions (Fig. 9G), and I just focused on a remarkable phenotype in the eye formation in this paper.

It has recently been proposed that a region near the NPC is transcriptionally active by forming the direct and dynamic link between an activated gene and the NPC, as shown in yeast and *Drosophila*, and humans (Brown et al., 2008; Mendjan et al., 2006; Taddei et al., 2006). Therefore, it will be interesting to examine whether Nemp1 is involved in this dynamic process of gene regulation near the NPC. As a next step, it is important to search and analyze Nemp1-interacting proteins in vertebrates to elucidate the mechanism involving INM proteins in developmental gene regulation.

Experimental procedures

cDNA cloning, sequence analysis, and constructs

cDNA library construction and screening were previously described (Osada et al., 2003; Takahashi et al., 2005). A full-length cDNA clone, pBluescript II-SK(–)*nemp1* [SK(–)*nemp1a*; DDBJ accession no. AB474919] was isolated from an ANE library (Takahashi et al., 2005). A alloallele gene, *nemp1b* (clone XL436g07ex; DDBJ accession no. AB474920), and *baf* alloallele genes, *baf-a* (clone XL456h02ex) and *baf-b* (clone XL455o03ex), were identified in a *Xenopus* EST database of NBRP (http://www.nbrp.jp/index.jsp), and were isolated from an ANE expression cDNA library (Osada et al., 2003). Computational sequence analyses were done using SignalP (http://www.cbs.dtu.dk/services/SignalP/) (Bendtsen et al., 2004), SMART (http://smart.embl-heidelberg.de/), TMHMM (http://www.cbs.dtu.dk/services/TMHMM/) (Krogh et al., 2001), Pfam (http://www.sanger.ac.uk/Software/Pfam/), and the NCBI conserved domain database (http://www.ncbi.nlm.nih.gov/Structure/cdd/cdd.shtml). Plasmid constructs were made with pCS107, pCS2+Myc, and pCS2+mcs4HAmcs as vectors at the *Bam*HI site for full-length Nemp1 [amino acid numbers (aa) 1–434], ΔN (lacking aa 37–175), 3TMs (lacking aa 232–317), 4TMs, (lacking aa 265–317), ΔA (lacking aa 176–287), ΔBt (aa 1–325), ΔSP (aa 35–434), ΔKR (lacking aa 317–325), ΔBBS (lacking aa 368-375), SPNA (aa 1–287), SP+TMs (aa 1–34 plus 149–317), ΔTMs (lacking aa 149–317), SP+A (aa 1–36 plus 176–287), SP+Bt (aa 1–35 plus 326–434), Ct (aa 318–434), KR (aa 317–325), and Bt (aa 326–434). All Nemp1 constructs were C-

terminally tagged with five-repeat Myc or four-repeat HA, designated as Nemp1-Myc or Nemp1-HA, respectively, and so on, using pCS2+MT or pCS2+mcs4HAmcs as a vector. N- and C-terminally HA-tagged human Emerin (HAn-Emerin and Emerin-HAc, respectively) and internally HA-tagged *Xenopus* MAN1 (MAN1-HAi), in which four-repeat HA was inserted after aa 421 between the two transmembrane domains, were made with pCS2+MT-Emerin and pCS2+MT-MAN1 as PCR templates (Osada et al., 2003) and pCS2+mcs4HAmcs as a vector. N-terminally two-repeat FLAG-tagged BAF was made with *baf-b* and pCS2+2FTn2.

Xenopus embryo manipulation and mRNA microinjection

Xenopus embryos were artificial fertilization, dejellied, and incubated in 0.1x Steinberg's solution (Peng, 1991). Embryos were staged according to the normal table of Nieuwkoop and Faber (Nieuwkoop and Faber, 1967). Microinjection of synthetic mRNA was done with a fine glass capillary and a pneumatic pressure injector IM300 (Narishige) in 3% Ficoll in 1x Modified Bath's solution (Peng, 1991). Injected embryos were kept in 3% Ficoll in 1x Modified Bath's solution for 2–3 h, transferred into 0.1x Steinberg's solution containing 50 μg/ml gentamicin sulfate, and incubated until embryos reached the appropriate stages. For mRNA synthesis, plasmids were linearized with *Asc*I or *Not*I and transcribed with SP6 polymerase (MEGAscript, Ambion) as described (Suga et al., 2006). mRNAs were injected into the dorsal blastomere of four cell-stage embryos. Nuclear β-*galactosidase* (nβ-*gal*) mRNA (60 pg/embryo) was coinjected for lineage tracing.

Whole-mount in situ hybridization and RT-PCR analysis

Whole-mount *in situ* hybridization (WISH) was performed according to Harland (Harland, 1991) using an automated system (AIH-201, Aloka). An antisense *nemp1a* and *baf-b* RNA probes were transcribed with T7 RNA polymerase from *Bam*HI-linearized SK(–)*nemp1* and a *baf-b* PCR product, which was amplified from pCS105-*baf-b* with the SP6 primer and a T7 promoter containing primer (5'-GTAATACGACTCACTATAGGGCGAGAGGCTC-3'). Other RNA probes were synthesized according to plasmid providers. RT-PCR was performed as described (Suga et al., 2006), with primer sets of *nemp1a* were forward, 5'-GAGGAGGCTGTAGAGTTAGT-3'; and reverse, 5'-GGACCACTTTACCTTCATAG-3', 29 cycles and *Histone H4* were forward, 5'-CGGGATAACATTCAGGGTATCACT-3', and reverse, 5'-ATCCATGGCGGTAACTGTCTTCCT-3' (Niehrs et al., 1994) (25 cycles).

Immunofluorescence microscopy

COS7 cells were grown in Dulbecco's modified Eagle's (DME) medium containing 10% fetal bovine serum. For transfection, cells were grown to almost 80% confluence and transfected with pCS2 expression constructs using FuGENE 6 Transfection Reagent (Roche). After 36-hour incubation, transfected cells were washed twice with phosphate-buffered saline (PBS) and fixed with 2% paraformaldehyde in PBS for 15 minutes at room temperature. Fixed cells were then permeabilized with 0.5% Triton-X 100 in PBS for 10

minutes, blocked in PBS containing 10% lamb serum for 1 hour at room temperature, and incubated with primary antibody in Tris-buffered saline (10 mM Tris-HCl, pH 7.5, 150 mM NaCl) containing 0.01% Tween 20 (TBS-T) for 1 hour at 37°C. Mouse anti-Myc 9E10 (BIOMOL; used at 1:1000), mouse anti-FLAG M2 (Sigma; used at 1:250), and rabbit anti-HA Y-11 (Santa Cruz; used at 1:200) antibodies were used as primary antibodies. After washing three times with TBS-T, the cells were incubated with Alexa 488-conjugated goat anti-mouse IgG, Alexa 546-conjugated goat anti-mouse IgG, and Alexa 555-conjugated goat anti rabbit IgG antibodies (Molecular Probes) at a concentration of 5 μg/ml as secondary antibody. Nuclei were stained with SytoxGreen (Molecular Probes). Digitonin extraction of fixed cells was done with 40 μg/ml digitonin (Wako) in PBS for 3 min on ice, and digitonin-treated cells were blocked in 0.5% gelatin in PBS for 15 min (Brachner et al., 2005) and in 10% lamb serum in PBS for 1 h at room temperature. Fixed *Xenopus* embryos were permeabilized and blocked with 0.1% Triton X-100 and 0.2% BSA, and 10% lamb serum in Tris-buffered saline (pH. 7.5) at room temperature. Confocal microscopic analysis with LSM Pascal (Zeiss) was performed as described (Osada et al., 2003).

Knockdown experiments

Antisense morpholino oligos, MOa and MOb, against exon 1 – intron 1 boundary sequences of *nemp1* alloalleles, *nemp1a* and *nemp1b*, were obtained from Gene Tools, LLC (MOa, 5'-TTTAAATTACCTGAGGCCAATGTAC-3'; MOb, 5'-ACACTTTATGTTATATTACGTGTCC-3'). Five mismatched MO (5mmMO, 5'-

ACAgTTTATcTTAaATTACgTGTgC-3'; lower cases are mismatched with MOb) was used as negative control. Prior to designing MOa and MOb, RNA splice junctions for *nemp1a* and *nemp1b* were identified by alignment of cDNA sequences with the *Xenopus/Silurana tropicalis* genome sequence (http://genome.jgi-psf.org/Xentr3/Xentr3.home.html). *nemp1a* and *nemp1b* genomic DNA fragments were PCR-amplified with *Xenopus laevis* genomic DNA and primers specific to exons 1 and 2 (5'-GAGGAGGCTGTAGAGTTAGT-3' and 5'-CGGACCACTTTACCTTCATAG-3' from the *Nemp1a* gene, respectively) and sequenced. MOa and MOb were dissolved in water and injected into the dorsal blastomere of four cell-stage embryos.

Glutathione S-transferase (GST) pull-down assay and western blotting

The C-terminal region of Nemp1 (Bt; aa 325-434) and the Bt lacking the BBS (BtΔBBS; aa 325-434 lacking aa 368–375) were subcloned into the pGEX-6P-1 vector to produce the GST-Bt and GST-BtΔBBS fusion proteins. Generation of GST fusion proteins was carried out as described previously (Hiratani et al., 2003; Osada et al., 2003). mRNA for FLAG-BAF was injected into the animal pole region of two-cell stage embryos. Injected embryos were cultured until the gastrula (stage 10.5), homogenized in 1x lysis buffer (20 mM Tris-HCl, pH 8.0, 1 mM EDTA, 10% glycerol, 8 mM DTT, 40 μg/ml leupeptin, 20 μg/ml aprotinin, 1 mM PMSF) containing 0.1% NP-40. Ten μg of purified GST, GST-MAN1-Ct, GST-Bt, or GST-BtΔBBS proteins bound to glutathione Sepharose 4B beads (GE Healthcare) was incubated with 150 μl of lysate of injected embryos for 1 h at 4°C. Subsequently, the Sepharose bead suspensions were washed with 1x lysis buffer.

Bound proteins were eluted by boiling in 2x SDS sample buffer, separated by SDS-PAGE (12.5% gel), and analyzed by western blotting with anti-FLAG M2 antibody (Sigma) or by Coomassie brilliant blue (CBB) staining. Western blotting was performed essentially as described (Shibata et al., 2005).

Acknowledgements

I wish to express my deep gratitude to Dr. Masanori Taira, Department of Biological Sciences, Graduate school of Science, The University of Tokyo. I thank K. Takeshima for *tbx3*; M. Jamrich for *rx2A*; P. Good for *nrp1*; Y. Sasai and K. Mizuseki for *sox2*; S. Tsukahara for *emerin*; D. Turner, R. Rupp, and J. Lee for pCS2+, pCS2+MT, and pCS2+nβ-gal; K. Miyazono and T. Mochizuki for COS-7 cells; T. Shiroishi for *X. laevis* genomic DNA; S. Matsuda for pCS2+mcs4HAmcs; K. Ogawa for pCS2+2FTn2; S. Taira for section examination, and S.-I. Osada for critical reading of the manuscript. National BioResource Project (NBRP) for EST clones (XL436g07ex, XL456h02ex, and XL455o03ex). I also thank Mr. Noriyuki Takahashi and all the member of the Laboratory of Molecular Biology for helpful comments and Discussions. This work was supported in part by the 21st Century COE Program of the Ministry of Education, Science, Sports, and Culture of Japan; and by Global COE program (Integrative Life Science Based on the Study of Biosignaling Mechanisms), MEXT, Japan.

References

Adam, S. A., Marr, R. S., Gerace, L., 1990. Nuclear protein import in permeabilized mammalian cells requires soluble cytoplasmic factors. J. Cell Biol. 111**,** 807-16.

Andreazzoli, M., Gestri, G., Angeloni, D., Menna, E., Barsacchi, G., 1999. Role of Xrx1 in Xenopus eye and anterior brain development. Development. 126**,** 2451-60.

Bailey, T. J., El-Hodiri, H., Zhang, L., Shah, R., Mathers, P. H., Jamrich, M., 2004. Regulation of vertebrate eye development by Rx genes. Int. J. Dev. Biol. 48**,** 761-70.

Bendtsen, J. D., Nielsen, H., von Heijne, G., Brunak, S., 2004. Improved prediction of signal peptides: SignalP 3.0. J. Mol. Biol. 340**,** 783-95.

Bengtsson, L., Wilson, K. L., 2004. Multiple and surprising new functions for emerin, a nuclear membrane protein. Curr. Opin. Cell Biol. 16**,** 73-9.

Bergametti, F., Denier, C., Labauge, P., Arnoult, M., Boetto, S., Clanet, M., Coubes, P., Echenne, B., Ibrahim, R., Irthum, B., et al., 2005. Mutations within the programmed cell death 10 gene cause cerebral cavernous malformations. Am J Hum Genet. 76**,** 42-51.

Bernier, G., Panitz, F., Zhou, X., Hollemann, T., Gruss, P., Pieler, T., 2000. Expanded retina territory by midbrain transformation upon overexpression of Six6 (Optx2) in Xenopus embryos. Mech. Dev. 93**,** 59-69.

Brachner, A., Reipert, S., Foisner, R., Gotzmann, J., 2005. LEM2 is a novel MAN1-related inner nuclear membrane protein associated with A-type lamins. J. Cell Sci. 118**,** 5797-810.

Brown, C. R., Kennedy, C. J., Delmar, V. A., Forbes, D. J., Silver, P. A., 2008. Global

histone acetylation induces functional genomic reorganization at mammalian nuclear pore complexes. Genes Dev. 22**,** 627-39.

Burke, B., Stewart, C. L., 2002. Life at the edge: the nuclear envelope and human disease. Nat. Rev. Mol. Cell. Biol. 3**,** 575-85.

Cai, M., Huang, Y., Suh, J. Y., Louis, J. M., Ghirlando, R., Craigie, R., Clore, G. M., 2007. Solution NMR structure of the barrier-to-autointegration factor-Emerin complex. J. Biol. Chem. 282**,** 14525-35.

Cai, M., Huang, Y., Zheng, R., Wei, S. Q., Ghirlando, R., Lee, M. S., Craigie, R., Gronenborn, A. M., Clore, G. M., 1998. Solution structure of the cellular factor BAF responsible for protecting retroviral DNA from autointegration. Nat. Struct. Biol. 5**,** 903-9.

Chow, R. L., Altmann, C. R., Lang, R. A., Hemmati-Brivanlou, A., 1999. Pax6 induces ectopic eyes in a vertebrate. Development. 126**,** 4213-22.

Chuang, J. C., Raymond, P. A., 2001. Zebrafish genes rx1 and rx2 help define the region of forebrain that gives rise to retina. Dev. Biol. 231**,** 13-30.

Chuang, J. C., Raymond, P. A., 2002. Embryonic origin of the eyes in teleost fish. BioEssays. 24**,** 519-29.

Danno, H., Michiue, T., Hitachi, K., Yukita, A., Ishiura, S., Asashima, M., 2008. Molecular links among the causative genes for ocular malformation: Otx2 and Sox2 coregulate Rax expression. Proc. Natl. Acad. Sci. USA. 105**,** 5408-13.

De Robertis, E. M., Larrain, J., Oelgeschlager, M., Wessely, O., 2000. The establishment of Spemann's organizer and patterning of the vertebrate embryo. Nat. Rev. Genet. 1**,** 171-81.

Dreger, M., Bengtsson, L., Schoneberg, T., Otto, H., Hucho, F., 2001. Nuclear envelope

proteomics: novel integral membrane proteins of the inner nuclear membrane. Proc. Natl. Acad. Sci. USA. 98**,** 11943-8.

Eagleson, G., Ferreiro, B., Harris, W. A., 1995. Fate of the anterior neural ridge and the morphogenesis of the Xenopus forebrain. J. Neurobiol. 28**,** 146-58.

Esteve, P., Bovolenta, P., 2006. Secreted inducers in vertebrate eye development: more functions for old morphogens. Curr. Opin. Neurobiol. 16**,** 13-9.

Furukawa, K., 1999. LAP2 binding protein 1 (L2BP1/BAF) is a candidate mediator of LAP2-chromatin interaction. J. Cell Sci. 112 (Pt 15)**,** 2485-92.

Giot, L., Bader, J. S., Brouwer, C., Chaudhuri, A., Kuang, B., Li, Y., Hao, Y. L., Ooi, C. E., Godwin, B., Vitols, E., et al., 2003. A protein interaction map of Drosophila melanogaster. Science. 302**,** 1727-36.

Griffis, E. R., Xu, S., Powers, M. A., 2003. Nup98 localizes to both nuclear and cytoplasmic sides of the nuclear pore and binds to two distinct nucleoporin subcomplexes. Mol. Biol. Cell. 14**,** 600-10.

Gruenbaum, Y., Margalit, A., Goldman, R. D., Shumaker, D. K., Wilson, K. L., 2005. The nuclear lamina comes of age. Nat. Rev. Mol. Cell. Biol. 6**,** 21-31.

Harland, R. M., In situ hybridization: an improved whole-mount method for Xenopus embryos. In: B. K. Kay, H. B. Peng, Eds.), Methods Cell Biol., Vol. 36. Academic Press, San Diego, CA, 1991, pp. 685-695.

He, M., Wen, L., Campbell, C. E., Wu, J. Y., Rao, Y., 1999. Transcription repression by Xenopus ET and its human ortholog TBX3, a gene involved in ulnar-mammary syndrome. Proc. Natl. Acad. Sci. USA. 96**,** 10212-7.

Hieda, M., Isokane, M., Koizumi, M., Higashi, C., Tachibana, T., Shudou, M., Taguchi, T., Hieda, Y., Higashiyama, S., 2008. Membrane-anchored growth factor, HB-EGF, on

the cell surface targeted to the inner nuclear membrane. J. Cell Biol. 180**,** 763-9.

Hill, R. E., Favor, J., Hogan, B. L., Ton, C. C., Saunders, G. F., Hanson, I. M., Prosser, J., Jordan, T., Hastie, N. D., van Heyningen, V., 1991. Mouse small eye results from mutations in a paired-like homeobox-containing gene. Nature. 354**,** 522-5.

Hiratani, I., Yamamoto, N., Mochizuki, T., Ohmori, S. Y., Taira, M., 2003. Selective degradation of excess Ldb1 by Rnf12/RLIM confers proper Ldb1 expression levels and Xlim-1/Ldb1 stoichiometry in Xenopus organizer functions. Development. 130**,** 4161-75.

Hirsch, N., Harris, W. A., 1997. Xenopus Pax-6 and retinal development. J. Neurobiol. 32**,** 45-61.

Hutchison, C. J., 2002. Lamins: building blocks or regulators of gene expression? Nat. Rev. Mol. Cell. Biol. 3**,** 848-58.

Inoue, T., Nakamura, S., Osumi, N., 2000. Fate mapping of the mouse prosencephalic neural plate. Dev. Biol. 219**,** 373-83.

Ishimura, A., Ng, J. K., Taira, M., Young, S. G., Osada, S., 2006. Man1, an inner nuclear membrane protein, regulates vascular remodeling by modulating transforming growth factor {beta} signaling. Development. 133**,** 3919-28.

King, M. C., Patrick Lusk, C., Blobel, G., 2006. Karyopherin-mediated import of integral inner nuclear membrane proteins. Nature. 442**,** 1003-7.

Knecht, A. K., Good, P. J., Dawid, I. B., Harland, R. M., 1995. Dorsal-ventral patterning and differentiation of noggin-induced neural tissue in the absence of mesoderm. Development. 121**,** 1927-35.

Krogh, A., Larsson, B., von Heijne, G., Sonnhammer, E. L., 2001. Predicting transmembrane protein topology with a hidden Markov model: application to

complete genomes. J. Mol. Biol. 305**,** 567-80.

Lagutin, O. V., Zhu, C. C., Kobayashi, D., Topczewski, J., Shimamura, K., Puelles, L., Russell, H. R., McKinnon, P. J., Solnica-Krezel, L., Oliver, G., 2003. Six3 repression of Wnt signaling in the anterior neuroectoderm is essential for vertebrate forebrain development. Genes Dev. 17**,** 368-79.

Lange, A., Mills, R. E., Lange, C. J., Stewart, M., Devine, S. E., Corbett, A. H., 2007. Classical nuclear localization signals: definition, function, and interaction with importin alpha. J. Biol. Chem. 282**,** 5101-5.

Lee, K. K., Haraguchi, T., Lee, R. S., Koujin, T., Hiraoka, Y., Wilson, K. L., 2001. Distinct functional domains in emerin bind lamin A and DNA-bridging protein BAF. J. Cell Sci. 114**,** 4567-73.

Li, H., Tierney, C., Wen, L., Wu, J. Y., Rao, Y., 1997. A single morphogenetic field gives rise to two retina primordia under the influence of the prechordal plate. Development. 124**,** 603-15.

Li, S., Armstrong, C. M., Bertin, N., Ge, H., Milstein, S., Boxem, M., Vidalain, P. O., Han, J. D., Chesneau, A., Hao, T., et al., 2004. A map of the interactome network of the metazoan C. elegans. Science. 303**,** 540-3.

Li, X., Perissi, V., Liu, F., Rose, D. W., Rosenfeld, M. G., 2002. Tissue-specific regulation of retinal and pituitary precursor cell proliferation. Science. 297**,** 1180-3.

Lin, F., Blake, D. L., Callebaut, I., Skerjanc, I. S., Holmer, L., McBurney, M. W., Paulin-Levasseur, M., Worman, H. J., 2000. MAN1, an inner nuclear membrane protein that shares the LEM domain with lamina-associated polypeptide 2 and emerin. J. Biol. Chem. 275**,** 4840-7.

Liu, J., Lee, K. K., Segura-Totten, M., Neufeld, E., Wilson, K. L., Gruenbaum, Y., 2003.

MAN1 and emerin have overlapping function(s) essential for chromosome segregation and cell division in Caenorhabditis elegans. Proc. Natl. Acad. Sci. USA. 100**,** 4598-603.

Liu, J., Rolef Ben-Shahar, T., Riemer, D., Treinin, M., Spann, P., Weber, K., Fire, A., Gruenbaum, Y., 2000. Essential roles for Caenorhabditis elegans lamin gene in nuclear organization, cell cycle progression, and spatial organization of nuclear pore complexes. Mol. Biol. Cell. 11**,** 3937-47.

Loosli, F., Winkler, S., Wittbrodt, J., 1999. Six3 overexpression initiates the formation of ectopic retina. Genes Dev. 13**,** 649-54.

Lupo, G., Andreazzoli, M., Gestri, G., Liu, Y., He, R. Q., Barsacchi, G., 2000. Homeobox genes in the genetic control of eye development. Int. J. Dev. Biol. 44**,** 627-36.

Mansharamani, M., Wilson, K. L., 2005. Direct binding of nuclear membrane protein MAN1 to emerin in vitro and two modes of binding to barrier-to-autointegration factor. J. Biol. Chem. 280**,** 13863-70.

Margalit, A., Brachner, A., Gotzmann, J., Foisner, R., Gruenbaum, Y., 2007. Barrier-to-autointegration factor--a BAFfling little protein. Trends Cell Biol. 17**,** 202-8.

Markiewicz, E., Tilgner, K., Barker, N., van de Wetering, M., Clevers, H., Dorobek, M., Hausmanowa-Petrusewicz, I., Ramaekers, F. C., Broers, J. L., Blankesteijn, W. M., et al., 2006. The inner nuclear membrane protein Emerin regulates beta-catenin activity by restricting its accumulation in the nucleus. EMBO J. 25**,** 3275-85.

Mathers, P. H., Grinberg, A., Mahon, K. A., Jamrich, M., 1997. The Rx homeobox gene is essential for vertebrate eye development. Nature. 387**,** 603-7.

Mendjan, S., Taipale, M., Kind, J., Holz, H., Gebhardt, P., Schelder, M., Vermeulen, M., Buscaino, A., Duncan, K., Mueller, J., et al., 2006. Nuclear pore components are

involved in the transcriptional regulation of dosage compensation in Drosophila. Mol. Cell. 21**,** 811-23.

Mizuseki, K., Kishi, M., Matsui, M., Nakanishi, S., Sasai, Y., 1998. Xenopus Zic-related-1 and Sox-2, two factors induced by chordin, have distinct activities in the initiation of neural induction. Development. 125**,** 579-87.

Montes de Oca, R., Lee, K. K., Wilson, K. L., 2005. Binding of barrier to autointegration factor (BAF) to histone H3 and selected linker histones including H1.1. J. Biol. Chem. 280**,** 42252-62.

Niehrs, C., 2004. Regionally specific induction by the Spemann-Mangold organizer. Nat. Rev. Genet. 5**,** 425-34.

Niehrs, C., Steinbeisser, H., De Robertis, E. M., 1994. Mesodermal patterning by a gradient of the vertebrate homeobox gene goosecoid. Science. 263**,** 817-20.

Nieuwkoop, P. D., Faber, J., 1967. Normal Table of Xenopus laevis (Daudin). North Holland, Amsterdam.

Oliver, G., Loosli, F., Koster, R., Wittbrodt, J., Gruss, P., 1996. Ectopic lens induction in fish in response to the murine homeobox gene Six3. Mech. Dev. 60**,** 233-9.

Osada, S.-I., Ohmori, S.-y., Taira, M., 2003. XMAN1, an inner nuclear membrane protein, antagonizes BMP signaling by interacting with Smad1 in *Xenopus* embryos. Development. 130**,** 1783-1794.

Ostlund, C., Ellenberg, J., Hallberg, E., Lippincott-Schwartz, J., Worman, H. J., 1999. Intracellular trafficking of emerin, the Emery-Dreifuss muscular dystrophy protein. J. Cell Sci. 112 (Pt 11)**,** 1709-19.

Pannese, M., Polo, C., Andreazzoli, M., Vignali, R., Kablar, B., Barsacchi, G., Boncinelli, E., 1995. The Xenopus homologue of Otx2 is a maternal homeobox gene that

demarcates and specifies anterior body regions. Development. 121**,** 707-20.

Peng, H. B., 1991. Xenopus laevis: Practical uses in cell and molecular biology. Solutions and protocols. Meth. Cell Biol. 36**,** 657-62.

Porter, F. D., Drago, J., Xu, Y., Cheema, S. S., Wassif, C., Huang, S. P., Lee, E., Grinberg, A., Massalas, J. S., Bodine, D., et al., 1997. Lhx2, a LIM homeobox gene, is required for eye, forebrain, and definitive erythrocyte development. Development. 124**,** 2935-44.

Schirmer, E. C., Florens, L., Guan, T., Yates, J. R., 3rd, Gerace, L., 2003. Nuclear membrane proteins with potential disease links found by subtractive proteomics. Science. 301**,** 1380-2.

Segura-Totten, M., Kowalski, A. K., Craigie, R., Wilson, K. L., 2002. Barrier-to-autointegration factor: major roles in chromatin decondensation and nuclear assembly. J. Cell Biol. 158**,** 475-85.

Shibata, M., Itoh, M., Hikasa, H., Taira, S., Taira, M., 2005. Role of crescent in convergent extension movements by modulating Wnt signaling in early Xenopus embryogenesis. Mech. Dev. 122**,** 1322-39.

Shinga, J., Itoh, M., Shiokawa, K., Taira, S., Taira, M., 2001. Early patterning of the prospective midbrain-hindbrain boundary by the HES-related gene XHR1 in Xenopus embryos. Mech. Dev. 109**,** 225-39.

Shumaker, D. K., Lee, K. K., Tanhehco, Y. C., Craigie, R., Wilson, K. L., 2001. LAP2 binds to BAF.DNA complexes: requirement for the LEM domain and modulation by variable regions. EMBO J. 20**,** 1754-64.

Soullam, B., Worman, H. J., 1993. The amino-terminal domain of the lamin B receptor is a nuclear envelope targeting signal. J. Cell Biol. 120**,** 1093-100.

Steventon, B., Carmona-Fontaine, C., Mayor, R., 2005. Genetic network during neural crest induction: from cell specification to cell survival. Semin. Cell Dev. Biol. 16**,** 647-54.

Suga, A., Hikasa, H., Taira, M., 2006. Xenopus ADAMTS1 negatively modulates FGF signaling independent of its metalloprotease activity. Dev. Biol. 295**,** 26-39.

Taddei, A., Van Houwe, G., Hediger, F., Kalck, V., Cubizolles, F., Schober, H., Gasser, S. M., 2006. Nuclear pore association confers optimal expression levels for an inducible yeast gene. Nature. 441**,** 774-8.

Takabatake, Y., Takabatake, T., Takeshima, K., 2000. Conserved and divergent expression of T-box genes Tbx2-Tbx5 in Xenopus. Mech. Dev. 91**,** 433-7.

Takada, H., Hattori, D., Kitayama, A., Ueno, N., Taira, M., 2005. Identification of target genes for the Xenopus Hes-related protein XHR1, a prepattern factor specifying the midbrain-hindbrain boundary. Dev. Biol. 283**,** 253-67.

Takahashi, N., Tochimoto, N., Ohmori, S.-y., Mamada, H., Itoh, M., Inamori, M., Shinga, J., Osada, S.-I., Taira, M., 2005. Systematic screening for genes specifically expressed in the anterior neuroectoderm during early Xenopus development. Int. J. Dev. Biol. 49**,** 939-951.

Tran, E. J., Wente, S. R., 2006. Dynamic nuclear pore complexes: life on the edge. Cell. 125**,** 1041-53.

Tsuchiya, Y., Hase, A., Ogawa, M., Yorifuji, H., Arahata, K., 1999. Distinct regions specify the nuclear membrane targeting of emerin, the responsible protein for Emery-Dreifuss muscular dystrophy. Eur. J. Biochem. 259**,** 859-65.

Tucker, P., Laemle, L., Munson, A., Kanekar, S., Oliver, E. R., Brown, N., Schlecht, H., Vetter, M., Glaser, T., 2001. The eyeless mouse mutation (ey1) removes an

alternative start codon from the Rx/rax homeobox gene. Genesis. 31**,** 43-53.

Varga, Z. M., Wegner, J., Westerfield, M., 1999. Anterior movement of ventral diencephalic precursors separates the primordial eye field in the neural plate and requires cyclops. Development. 126**,** 5533-46.

Wang, X., Xu, S., Rivolta, C., Li, L. Y., Peng, G. H., Swain, P. K., Sung, C. H., Swaroop, A., Berson, E. L., Dryja, T. P., et al., 2002. Barrier to autointegration factor interacts with the cone-rod homeobox and represses its transactivation function. J. Biol. Chem. 277**,** 43288-300.

Wilhelmsen, K., Litjens, S. H., Kuikman, I., Tshimbalanga, N., Janssen, H., van den Bout, I., Raymond, K., Sonnenberg, A., 2005. Nesprin-3, a novel outer nuclear membrane protein, associates with the cytoskeletal linker protein plectin. J. Cell Biol. 171**,** 799-810.

Wu, W., Lin, F., Worman, H. J., 2002. Intracellular trafficking of MAN1, an integral protein of the nuclear envelope inner membrane. J. Cell Sci. 115**,** 1361-71.

Yu, R. T., Chiang, M. Y., Tanabe, T., Kobayashi, M., Yasuda, K., Evans, R. M., Umesono, K., 2000. The orphan nuclear receptor Tlx regulates Pax2 and is essential for vision. Proc. Natl. Acad. Sci. USA. 97**,** 2621-5.

Zhang, Q., Ragnauth, C., Greener, M. J., Shanahan, C. M., Roberts, R. G., 2002. The nesprins are giant actin-binding proteins, orthologous to Drosophila melanogaster muscle protein MSP-300. Genomics. 80**,** 473-81.

Zuber, M. E., Gestri, G., Viczian, A. S., Barsacchi, G., Harris, W. A., 2003. Specification of the vertebrate eye by a network of eye field transcription factors. Development. 130**,** 5155-67.

Zuber, M. E., Perron, M., Philpott, A., Bang, A., Harris, W. A., 1999. Giant eyes in

Xenopus laevis by overexpression of XOptx2. Cell. 98**,** 341-52.

Figures

Fig. 1. A model of neural induction and patterning by the head and trunk organizers in the *Xenopus* embryo

During gastrulation, the Spemann organizer induces neural tissue from the overlying ectoderm by secreting BMP inhibitors, which are known as neural inducers (Left panel; sagittal view of the gastrula). The Spemann organizer is divided into the head and trunk organizers. The trunk organizer secretes posteriorizing factors, which include fibroblast growth factors (FGFs), Wnt proteins, and retinoic acid (RA), whereas the head organizer expresses or secretes inhibitors, such as the secreted Wnt inhibitors Dkk1, Frzb, and Crescent. In the neurula embryo, the neural plate is divided into the presumptive forebrain-midbrain region and hindbrain-spinal cord region, which correspond to the head and trunk organizer, respectively, in terms of the anteroposterior position (right panel; dorsal view of the neurula). The eye anlagen will be formed in the forebrain.

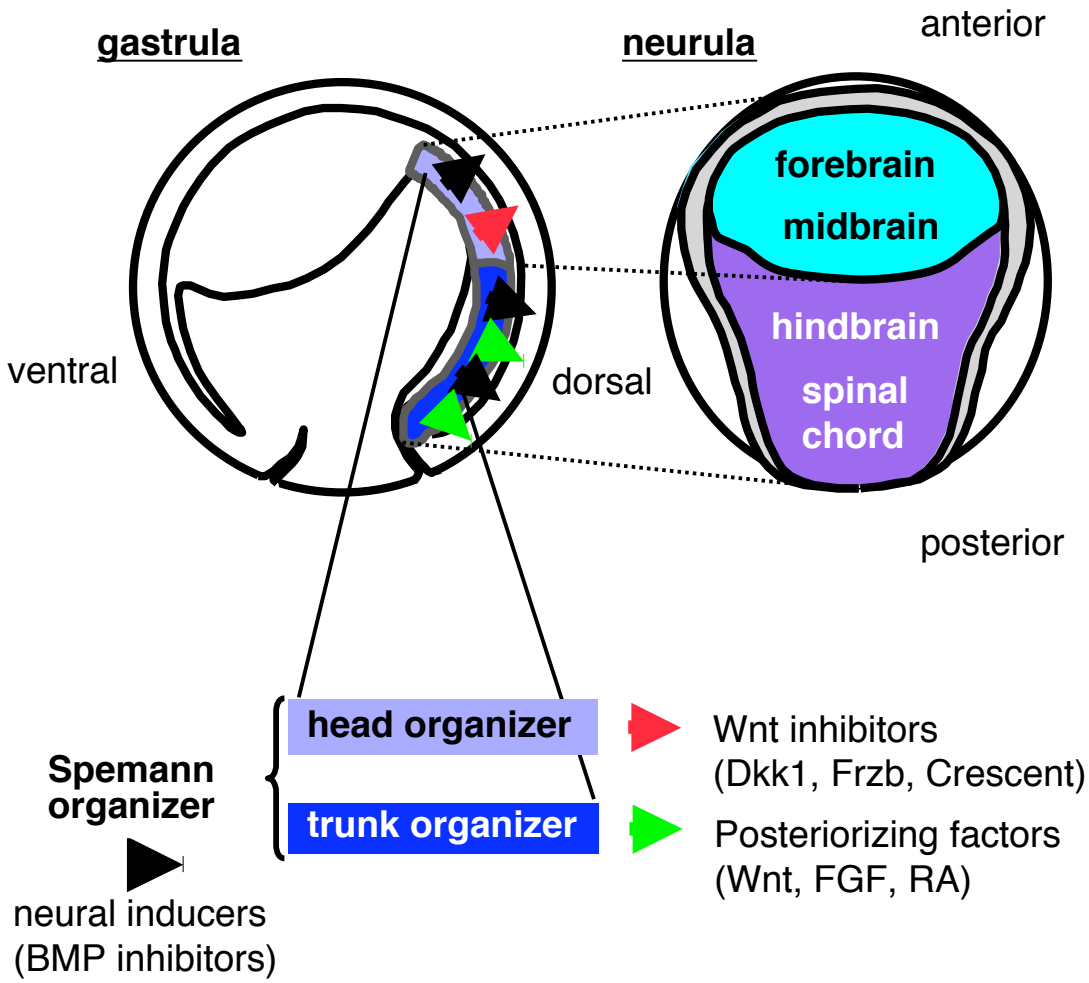
gastrula
neurula
anterior
forebrain
midbrain
hindbrain
spinal chord
ventral
dorsal
posterior
head organizer
trunk organizer
Spemann organizer
neural inducers (BMP inhibitors)
Wnt inhibitors (Dkk1, Frzb, Crescent)
Posteriorizing factors (Wnt, FGF, RA)

Figure 1

Fig. 2. Structure of the nuclear envelope and nuclear membrane proteins

The nuclear envelope (NE) has two membranes, inner and outer nuclear membranes (INM and ONM, respectively), which join to form 'pores' that are occupied by nuclear pore complexes (NPCs). For clarity, only two nuclear pores are depicted. NPCs mediate traffic in and out of the nucleus, as indicated by the double-headed arrows. The NE is continuous with the endoplasmic reticulum (ER) network. Integral INM proteins such as emerin (blue triangle), MAN1 (blue U-shape), and Lamin-binding protein (blue box) are shown. (Modified from Gruenbaum et al. (2005) *Nat. Rev. Mol. Cell Biol.* 6:21)

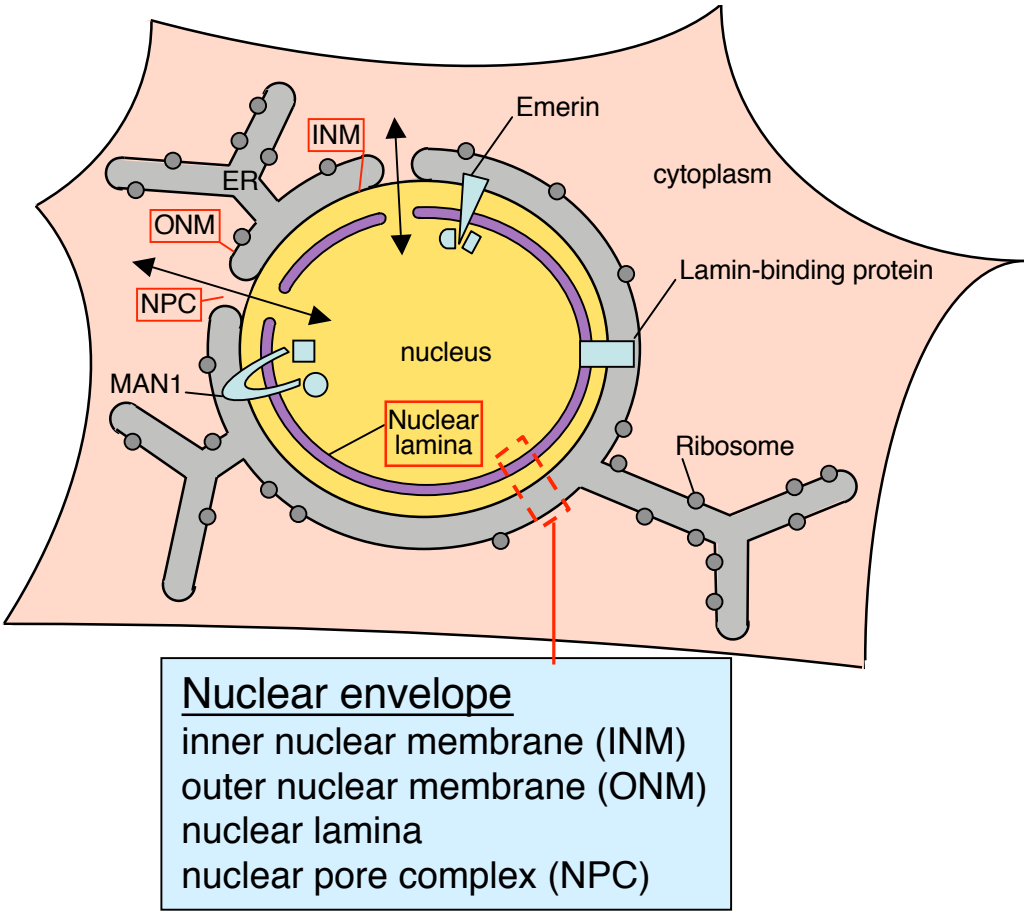

Nuclear envelope
inner nuclear membrane (INM)
outer nuclear membrane (ONM)
nuclear lamina
nuclear pore complex (NPC)

Figure 2

Fig. 3. A model of eye field formation in the anterior neural plate

The turquoise region indicates anterior neural plate, and the magenta region shows the eye field. (Modified from Zuber et al. (2003) *Development* 130:5155; and Danno et al. (2008) *PNAS.* 105:5408)

Gene expression pattern of eye development

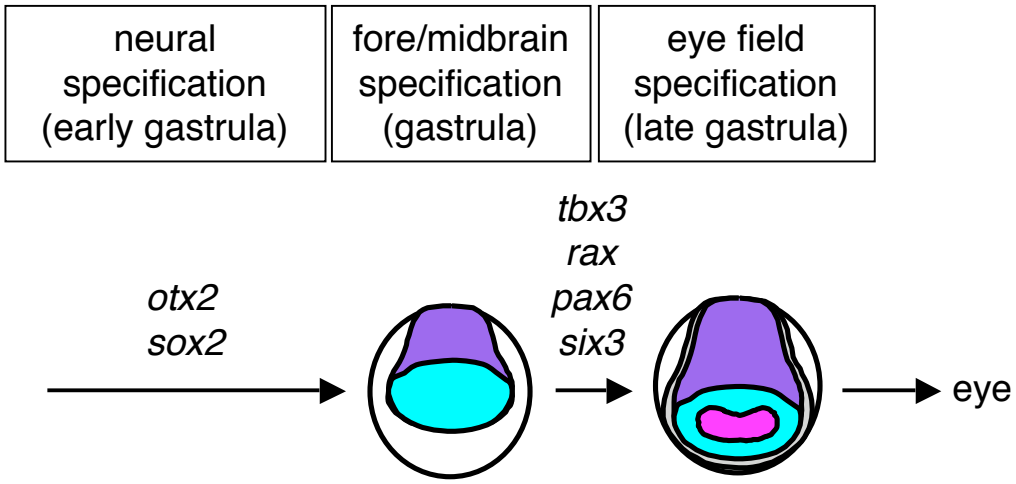

Functional interaction for eye development

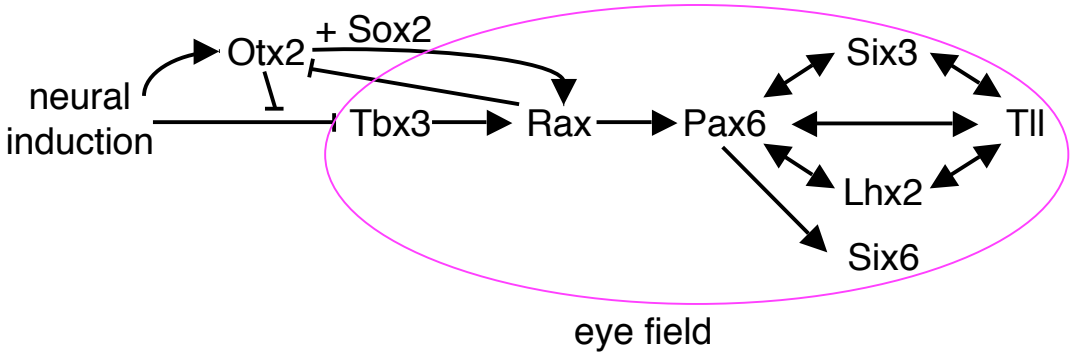

Figure 3

Fig. 4. Strategy for systematic screening of genes specifically expressed in the *Xenopus* anterior neuroectoderm.

Screening for eliminating non-specific clones in the ANE region from an ANE library was performed along this scheme. Dissection of late-gastrula (stage 12-12.5) embryos was performed for isolation of ANE and AEM (anterior endomesoderm) regions. Dissected pieces were treated with collagenase and separated into ANE and underlying AEM. A region-specific cDNA library was constructed from the ANE RNA. Further detailed processes are previously described (Takahashi et al., 2005). (Modified from Takahashi et al. (2005) *Int. J. Dev. Biol.* 49:939)

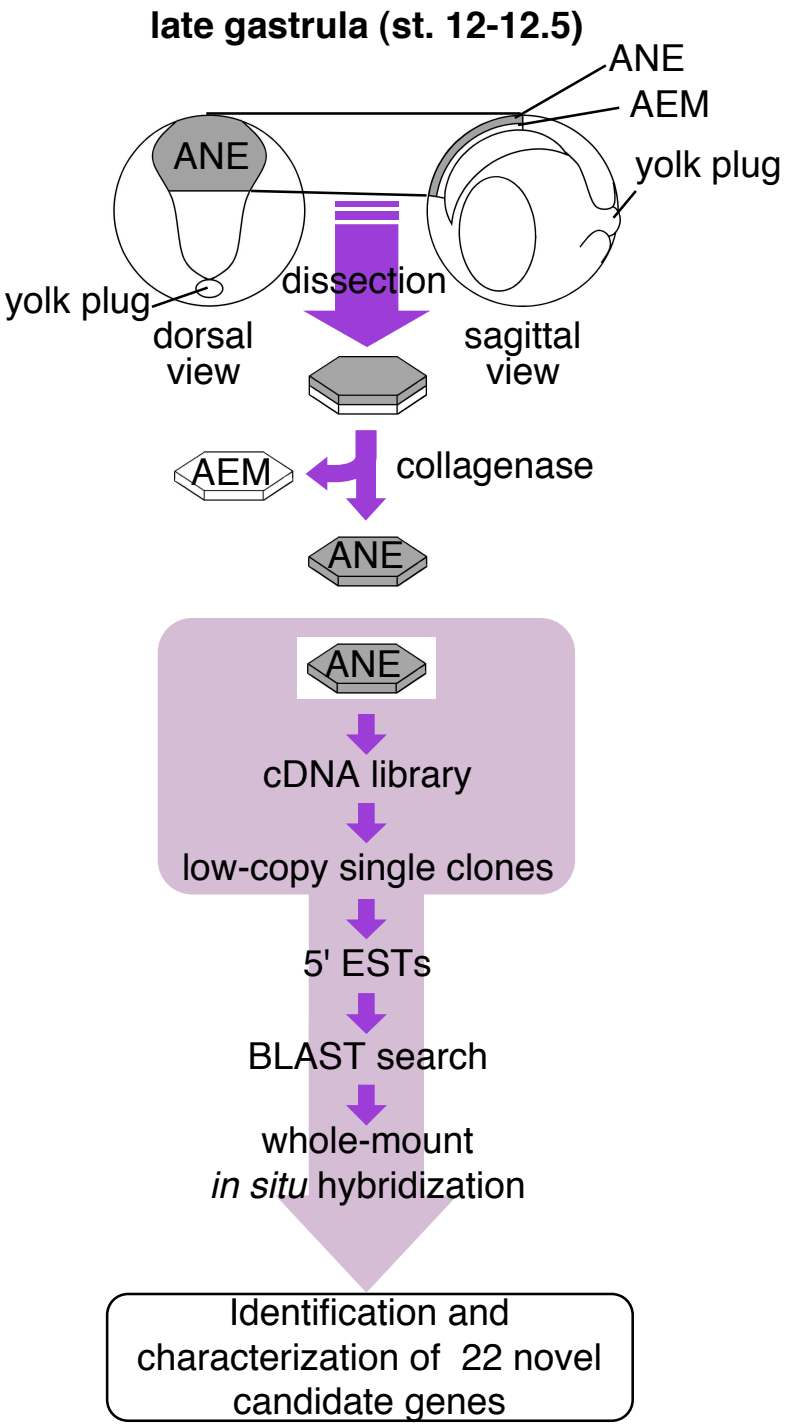
late gastrula (st. 12-12.5)
ANE
AEM
yolk plug
ANE
yolk plug
dissection
dorsal view
sagittal view
AEM
collagenase
ANE
ANE
cDNA library
low-copy single clones
5' ESTs
BLAST search
whole-mount
in situ hybridization
Identification and characterization of 22 novel candidate genes

Figure 4

Fig. 5. Amino acid sequence alignments of isolated clones and best hit proteins.

(A) N17D12 and human KIAA0286 (accession number, O14524). N17D12 has no domain or motifs.

(B) N20H12 and human Src-associated protein SAW (accession number, NP_115551). N20H12 has sixth WD40 domains (dark blue lines).

(C) N21E5 and human Proline-rich coiled-coil 1 (accession number, NP_570721). N21E5 has unknown conserved domain (green lines).

(D) N23G4 and human Glutaredoxin 5 (accession number, NP_057501). N23G4 has signal peptide (purple lines) and glutaredoxin domain (orange lines).

(E) N27F9 and human Programmed cell death 10 (accession number, NP_009148). N27F9 is highly conserved with Programmed cell death 10.

(F) N31A5 and human Similar to CG17293-PA (unknown protein) (accession number, XP_001127580). N31A5 has sixth WD40 domains (dark blue lines).

(G) N32C3 and human Zinc finger protein 668 (accession number, BAB55084). N32C3 has sixteenth C2H2 domains (light blue lines).

A

Upper : N17D12 (Nemp1a)
Middle: Nemp1b
Lower : human KIAA0286

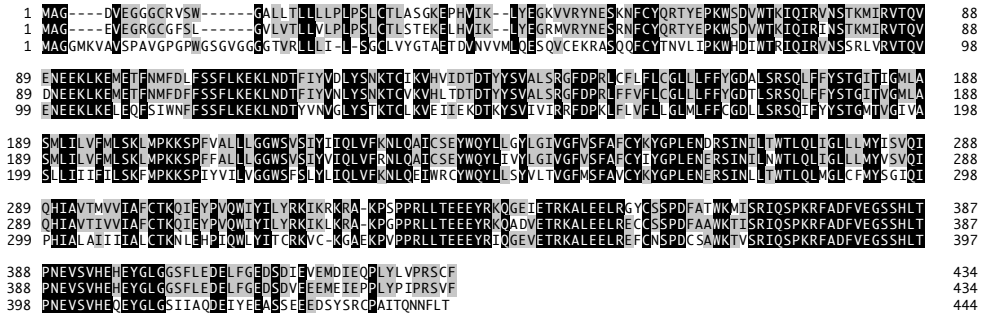

B

Upper: N20H12
Lower: human Src-associated protein SAW

C

Upper: N21E5
Lower: human Proline-rich coiled-coil 1

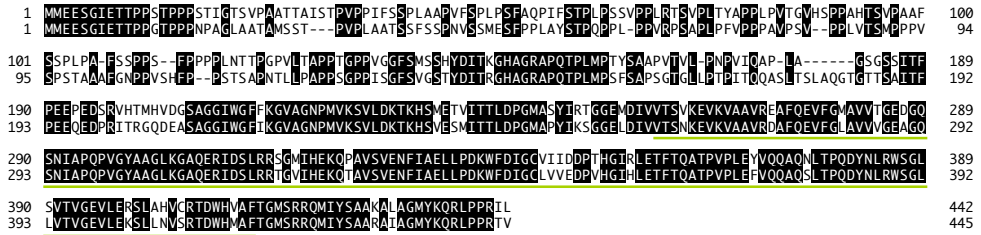

Figure 5

D

Upper: N23G4

Lower: human Glutaredoxin 5

E

Upper: N27F9

Lower: human Programmed cell death 10

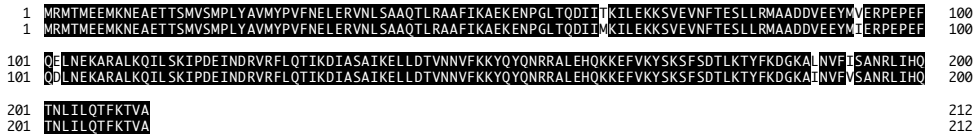

F

Upper: N31E5

Lower: human Similar to CG17293-PA

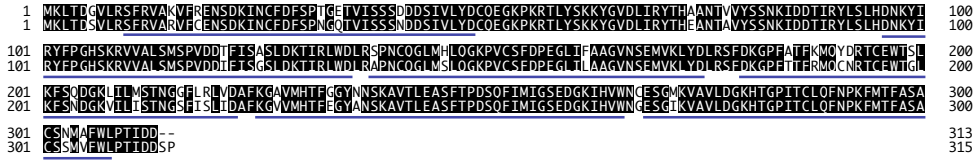

G

Upper: N32C3

Lower: human Zinc finger protein 668

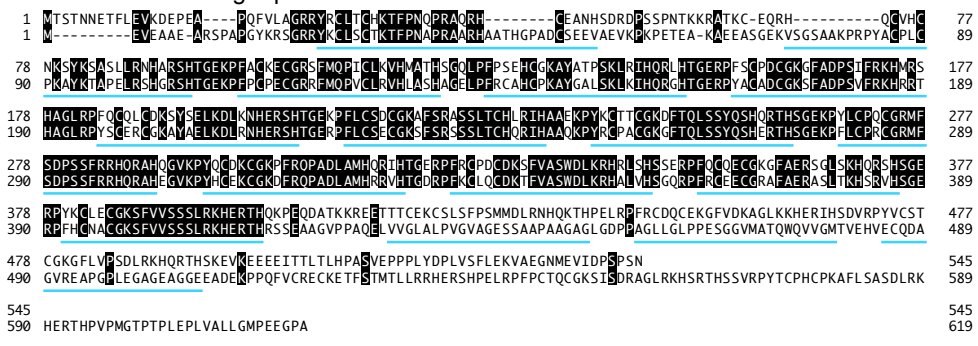

Figure 5 (continued)

Fig. 6. Confocal microscopic analysis for subcellular localization of Myc-tagged proteins.

Subcellular localization of C-terminally Myc-tagged constructs of seven possible novel genes was analyzed by immunostaining (red). Nuclear DNA was stained with SytoxGreen (green).

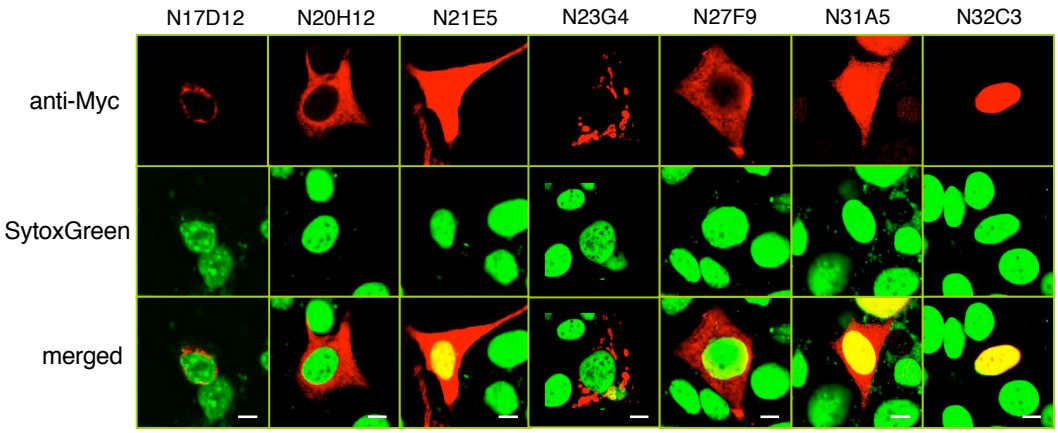
N17D12
N20H12
N21E5
N23G4
N27F9
N31A5
N32C3
anti-Myc
SytoxGreen
merged

Figure 6

Fig. 7. Structure of Nemp1.

(A) Amino acid sequence of *Xenopus* Nemp1. A putative SP (purple line), TMs (red letters) and a KR (yellow box), BBS (blue box), and evolutionary conserved Region A (pink line) and Region B (green line) are indicated. The arrowhead indicates a putative cleavage site of SP.

(B) Schematic structure and Kyte–Doolittle hydropathy plot of Nemp1. Color indications are the same as in A.

(C) Schematic structural comparison of Nemp1 and its possible orthologs. Percent identities of amino acid sequences against the *Xenopus* Nemp1a sequence are shown. Accession numbers of amino acid sequences: human, O14524; mouse, Q6ZQE4; zebrafish, XM_683418; ascidian (*Ciona intestinalis*), AK116477; *Drosophila*, NP_573142; and *C. elegans*, NP_497202.

A

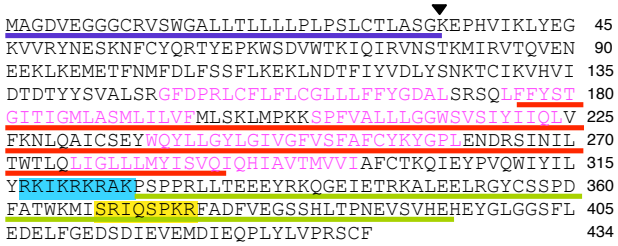
MAGDVEGGGCRVSWGALLTLLLLPLPSLCTLASGKEPHVIKLYEG 45
KVVRYNESKNFCYQRTYEPKWSDVWTKIQIRVNSTKMIRVTQVEN 90
EEKLKEMETFNMFDLFSSFLKEKLNDTFIYVDLYSNKTCIKVHVI 135
DTDTYYSVALSRGFDPRLCFLFLCGLLLFFYGDALSRSQLFFYST 180
GITIGMLASMLILVFMLSKLMPKKSPFVALLLGGWSVSIYIIQLV 225
FKNLQAICSEYWQYLLGYLGIVGFVSFAFCYKYGPLENDRSINIL 270
TWTLQLIGLLLMYISVQIQHIAVTMVVIAFCTKQIEYPVQWIYIL 315
YRKIKRKRAKPSPPRLLTEEEYRKQGEIETRKALEELRGYCSSPD 360
FATWKMISRIQSPKRFADFVEGSSHLTPNEVSVHEHEYGLGGSFL 405
EDELFGEDSDIEVEMDIEQPLYLVPRSCF 434

B

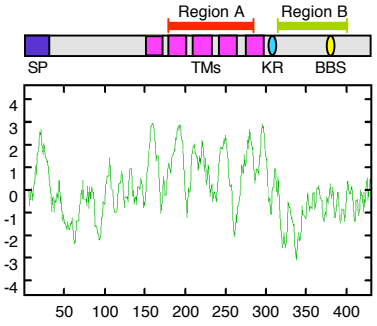
Region A
Region B
SP
TMs
KR
BBS
4
3
2
1
0
-1
-2
-3
-4
50
100
150
200
250
300
350
400

C

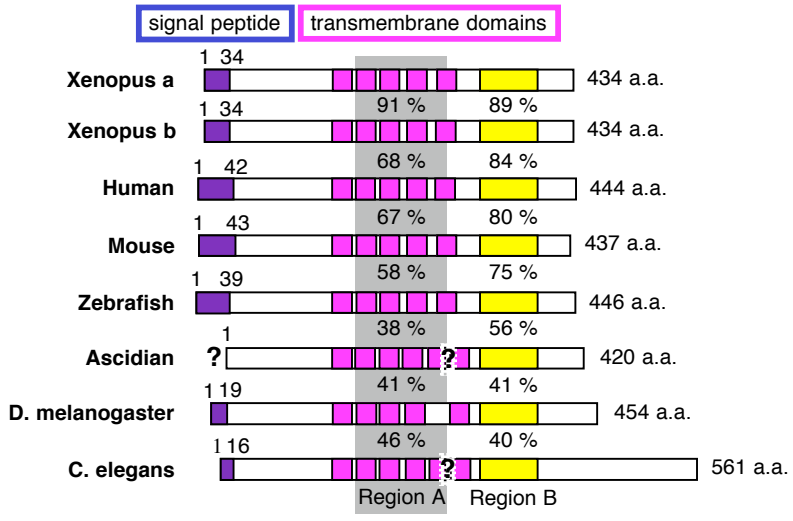
signal peptide
transmembrane domains
Xenopus a
1 34
434 a.a.
Xenopus b
1 34
91 %
89 %
434 a.a.
Human
1 42
68 %
84 %
444 a.a.
Mouse
1 43
67 %
80 %
437 a.a.
Zebrafish
1 39
58 %
75 %
446 a.a.
Ascidian
1
?
38 %
56 %
?
420 a.a.
D. melanogaster
1 19
41 %
41 %
454 a.a.
C. elegans
1 16
46 %
40 %
?
561 a.a.
Region A
Region B

Figure 7

Fig. 8. Subcellular localization of Nemp1.

(A) Confocal microscopic analysis of subcellular localization. Nemp1-Myc and MAN1-Myc were analyzed by immunostaining (red). Nuclear DNA was stained with SytoxGreen (green).

(B) Differential permeabilization of the ONM and INM with digitonin as assayed by HA-tagged MAN1 (MAN1-HAi). COS7 cells were cotransfected with expression constructs for Bt-Myc (green) and MAN1-HAi (red), and treated with digitonin for 1 to 25 min or with Triton X-100 (Triton) as indicated. Staining patters are classified as follows: type 1, cytoplasmic staining of Bt-Myc; type 2, ubiquitous staining of Bt-Myc; type A, partial NE staining of MAN1-HAi (less than 90% of the NE); type B, NE staining of MAN1-HAi (equal to or more than 90% of the NE). A bar graph shows percentages of combinatorial staining types in different colors as indicated below the pictures. A set of transfected cells was used to equalize transfection efficiency for all staining conditions. Experiments were repeated three times, and the results were reproducible. n, total number of transfected cells.

(C) Differential permeabilization of the ONM and INM with digitonin as assayed by HA-tagged Emerin (Emerin-HAc and HAn-Emerin). COS7 cells were cotransfected with expression constructs for Bt-Myc (green) and Emerin-HAc (red) or HAn-Emerin (red), and treated with digitonin for 3 min. See (B) for details.

(D) Schematic representation of nuclear membrane permeabilization with digitonin and Triton X-100. Red circle; bind to anti-body; white circle, not bind to anti-body; dotted line, permeabilized membrane; solid line, not permeabilized membrane.

(E) INM localization of Nemp1-HA. COS7 cells were cotransfected with expression constructs for Bt-Myc (green) and Nemp1-HA (red) or Nemp1-Myc (green) and HAn-Emerin (red) or Emerin-HAc (red), and treated with digitonin for 3 min. Dotted white circle, the position of NE (a). Note that weak cytoplasmic staining of Nemp1-HA (a), Nemp1-Myc (c,e), and HAn-Emerin (e) was detected, indicating successful transfection of expression constructs. Scale bars: 5 μm.

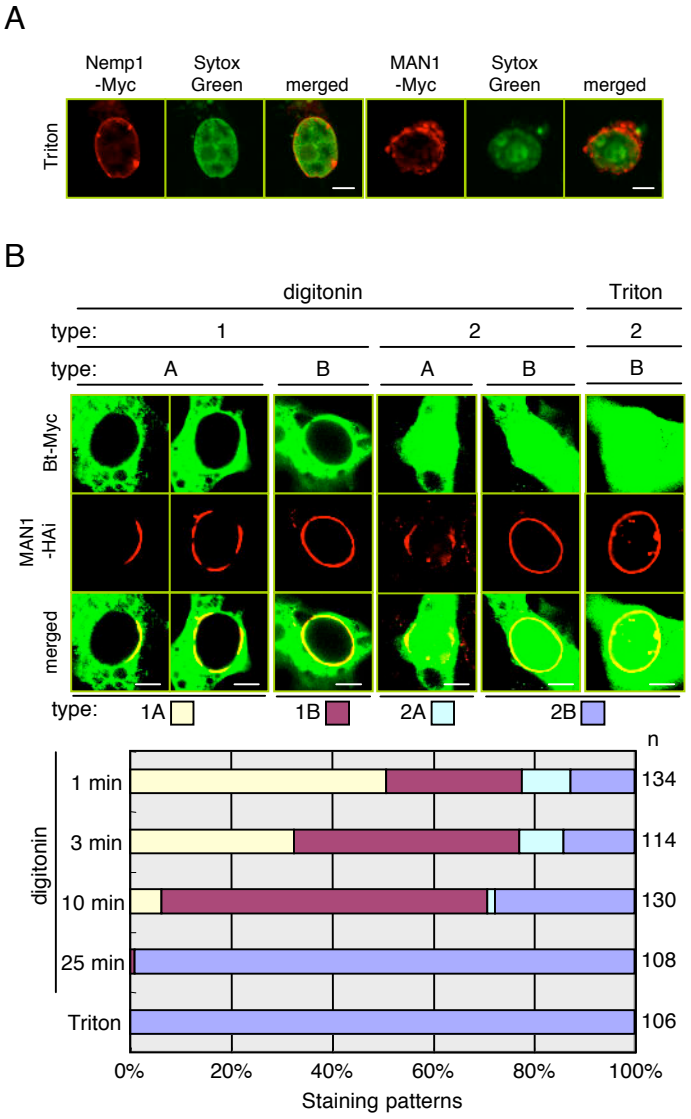
A
Nemp1
-Myc
Sytox
Green
merged
MAN1
-Myc
Sytox
Green
merged
Triton
B
digitonin
Triton
type:
1
2
2
type:
A
B
A
B
B
Bt-Myc
MAN1
-HAi
merged
type:
1A
1B
2A
2B
n
digitonin
1 min
3 min
10 min
25 min
Triton
134
114
130
108
106
0%
20%
40%
60%
80%
100%
Staining patterns

Figure 8

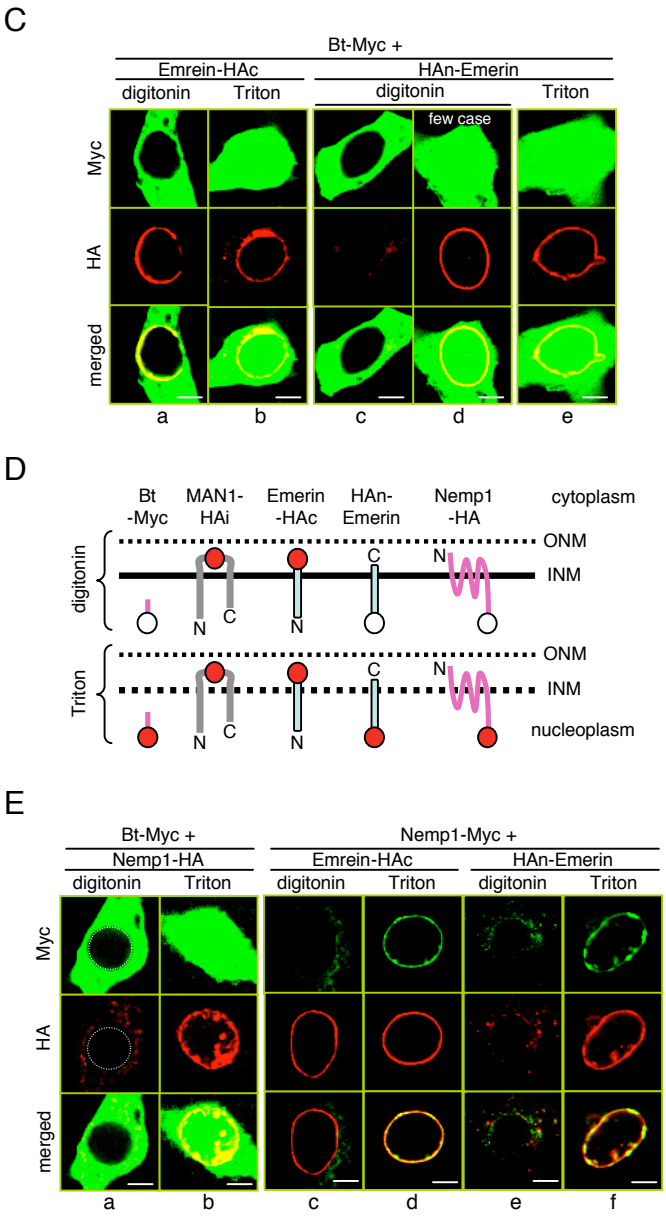

Figure 8 (continued)

Fig. 9. Spatiotemporal expression of *nemp1* and *baf*.

(A) RT-PCR analysis of *nemp1a* expression. Developmental stages are as indicated. *histone H4*, loading control.

(B, C) WISH analysis for *nemp1* (B) and *baf* (C). (Ba) Lateral view; (Bb) a hemisection of (Ba); (Bc,e and Ca,c) anterior view with the dorsal side up; (Bd,f and Cb,d) dorsal view with the anterior side up; (Bg and Ce) lateral view with the dorsal side up. opv, optic vesicle; otv, otic vesicle; ba, branchial arches.

(D) Section examination of the head region. Stained tailbud embryos (stage 28) were sectioned at the position of eyes. Nuclei were stained with DAPI. Arrowhead, diencephalon; arrow, optic vesicle.

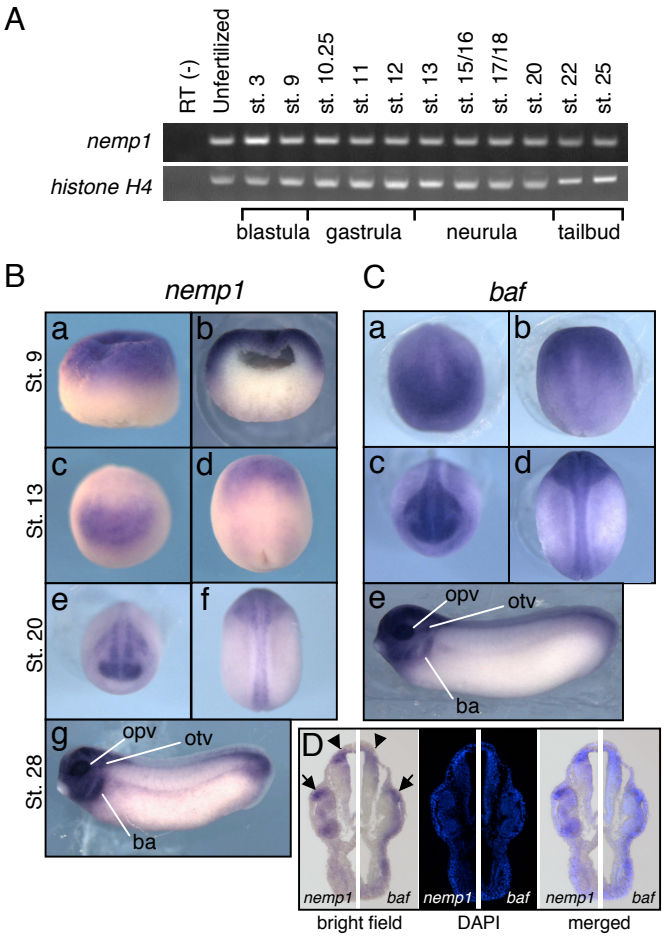
A
RT (-)
Unfertilized
st. 3
st. 9
st. 10.25
st. 11
st. 12
st. 13
st. 15/16
st. 17/18
st. 20
st. 22
st. 25
nemp1
histone H4
blastula
gastrula
neurula
tailbud
B
nemp1
C
baf
St. 9
St. 13
St. 20
St. 28
a
b
c
d
e
f
g
opv
otv
ba
D
nemp1
baf
bright field
DAPI
merged

Figure 9

Fig. 10. Overexpression of Nemp1 causes eye defects and reduces expression of eye marker genes at the neurula stage.

Embryos were injected with mRNA for Nemp1 or globin as indicated, together with nβ-*gal* mRNA.

(A) Eye-defect phenotypes at the tailbud stage (stages 40-41). Fractions indicate the proportion of the presented phenotype per total number of informative injected embryos.

(B) WISH analysis at the neurula stage (stages 13-14). Examined genes are as indicated. Numbers in red, downregulation; numbers in black, normal expression. ant, anterior view (dorsal is upwards); dor, dorsal view (anterior is upwards); arrowhead, injected side. Amounts of injected mRNAs (pg/embryo): *nemp1a*, 400; *globin*, 400.

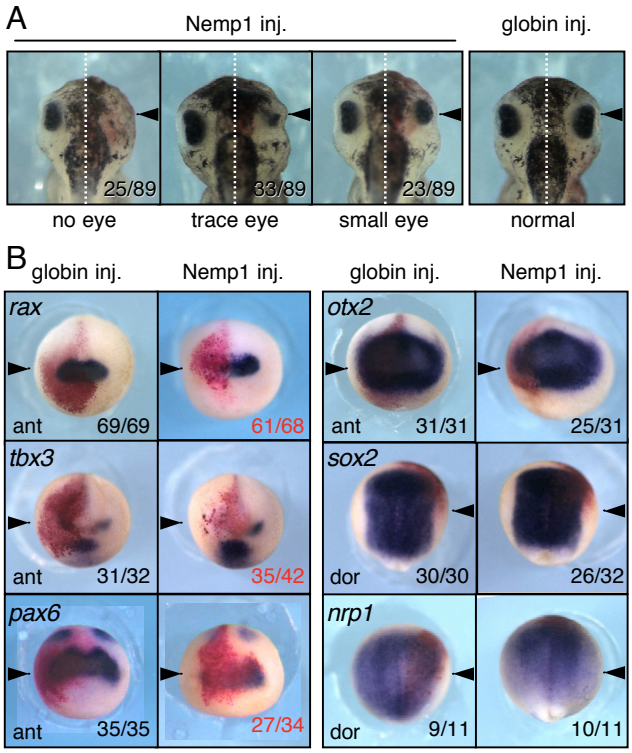
A
Nemp1 inj.
globin inj.
25/89
33/89
23/89
no eye
trace eye
small eye
normal
B
globin inj.
Nemp1 inj.
globin inj.
Nemp1 inj.
rax
ant
69/69
61/68
otx2
ant
31/31
25/31
tbx3
ant
31/32
35/42
sox2
dor
30/30
26/32
pax6
ant
35/35
27/34
nrp1
dor
9/11
10/11

Figure 10

Fig. 11. Knockdown of Nemp1 by MOab disrupts eye development.

(A) MOab inhibits splicing of *nemp1* pre-mRNA. (Upper panel) Sequence alignment of exon 1-intron 1 splice junctions. Target sequences of MOa and MOb are underlined. (Lower panel) RT-PCR detection of unspliced transcripts in MOab (25 or 50 ng) or 5mmMO (50 ng)-injected embryos. RT–, RT-PCR without reverse transcriptase reaction.
(B) Morphological appearances of injected embryos. MOab (Ba), 5mmMO (Bb), or MOab plus *nemp1* mRNA (Bc) were injected together with nβ-*gal* mRNA as a tracer (red) into the animal pole region of both right blastomeres at the four cell stage. Injected doses (per embryo): MOab 20 ng; *nemp1* mRNA, 200 pg. Upper panels, dorsal view (anterior is upwards); lower panels, right side view of the same embryo in the upper panels.
(C) WISH analysis of 5mmMO- or MOab-injected embryos at stages 13–14. Arrowhead, injected side.

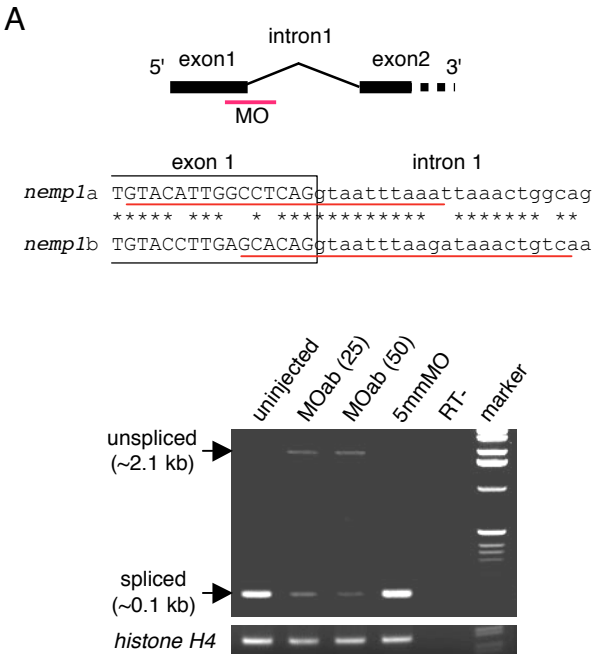
A
intron1
5'
exon1
exon2
3'
MO
exon 1
intron 1
nemp1a TGTACATTGGCCTCAGgtaatttaaattaaactggcag
***** *** * ********** ******* **
nemp1b TGTACCTTGAGCACAGgtaatttaagataaactgtcaa
uninjected
MOab (25)
MOab (50)
5mmMO
RT-
marker
unspliced
(~2.1 kb)
spliced
(~0.1 kb)
histone H4

Figure 11

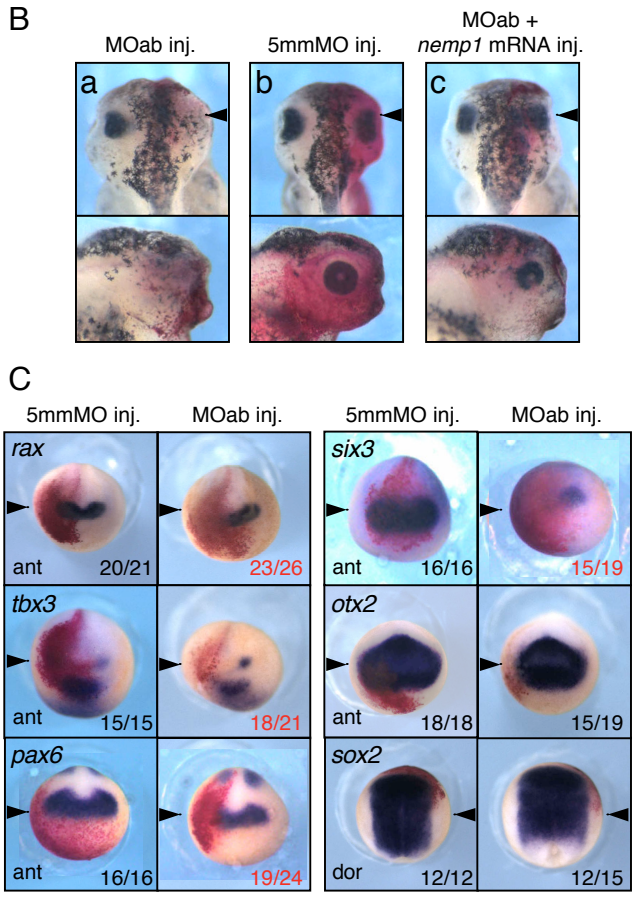

Figure 11 (continued)

Fig. 12. Rescue experiments for *nemp1* morphants using *pax6* and *rax* mRNA.

Embryos were coinjected with MOab and *pax6* or *rax* mRNA as indicated.

(A) Coinjection with *pax6* mRNA. Phenotypes were analyzed by WISH for *six3* expression.

(B) Coinjection with *rax* mRNA. Phenotypes were analyzed by WISH for *pax6* expression. Other experimental procedures were the same as in Fig. 11.

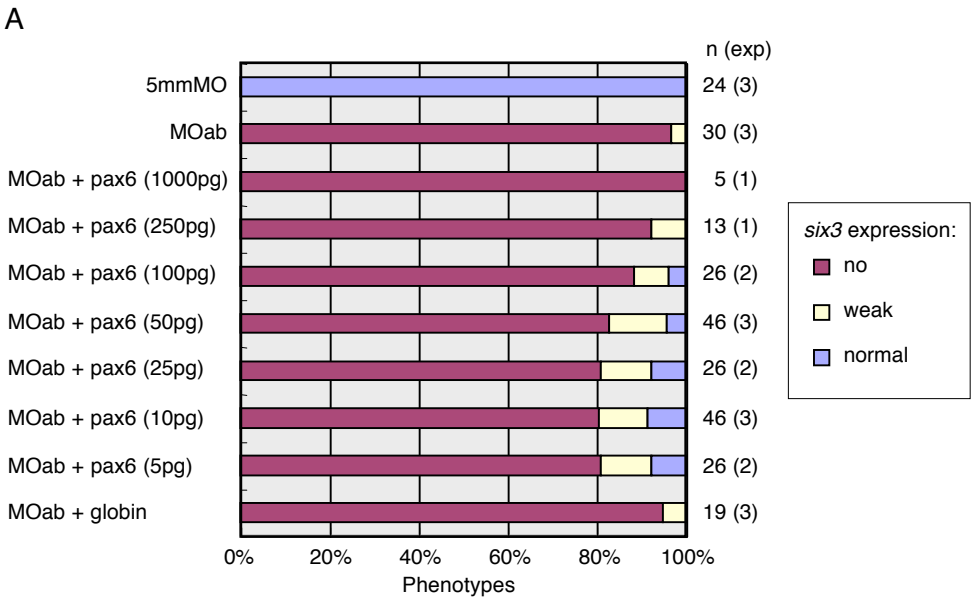
A
n (exp)
5mmMO
MOab
MOab + pax6 (1000pg)
MOab + pax6 (250pg)
MOab + pax6 (100pg)
MOab + pax6 (50pg)
MOab + pax6 (25pg)
MOab + pax6 (10pg)
MOab + pax6 (5pg)
MOab + globin
24 (3)
30 (3)
5 (1)
13 (1)
26 (2)
46 (3)
26 (2)
46 (3)
26 (2)
19 (3)
0%
20%
40%
60%
80%
100%
Phenotypes
six3 expression:
no
weak
normal

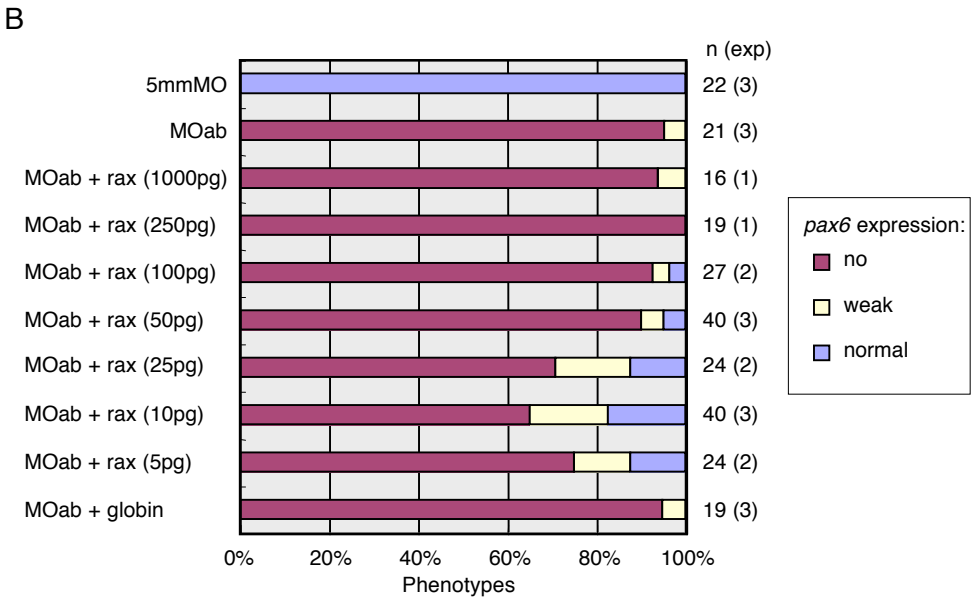
B
n (exp)
5mmMO
MOab
MOab + rax (1000pg)
MOab + rax (250pg)
MOab + rax (100pg)
MOab + rax (50pg)
MOab + rax (25pg)
MOab + rax (10pg)
MOab + rax (5pg)
MOab + globin
22 (3)
21 (3)
16 (1)
19 (1)
27 (2)
40 (3)
24 (2)
40 (3)
24 (2)
19 (3)
0%
20%
40%
60%
80%
100%
Phenotypes
pax6 expression:
no
weak
normal

Figure 12

Fig. 13. Activities of Nemp1-deletion constructs for eye development.

(A) Schematic representations of *nemp1* constructs.

(B) Activity of *nemp1* constructs for eye defect phenotypes. A bar graph shows percentages of eye defects at tailbud stages (stages 40–42) in embryo injected with mRNA as indicated. Colors of the bar correspond to those in upper panel (see Fig. 10A for eye phenotypes). n, total number of injected embryos; exp, number of independent experiments.

(C) Effects of Nemp1 and deletion mutants on *rax* expression in the neurula (stages 13–14).

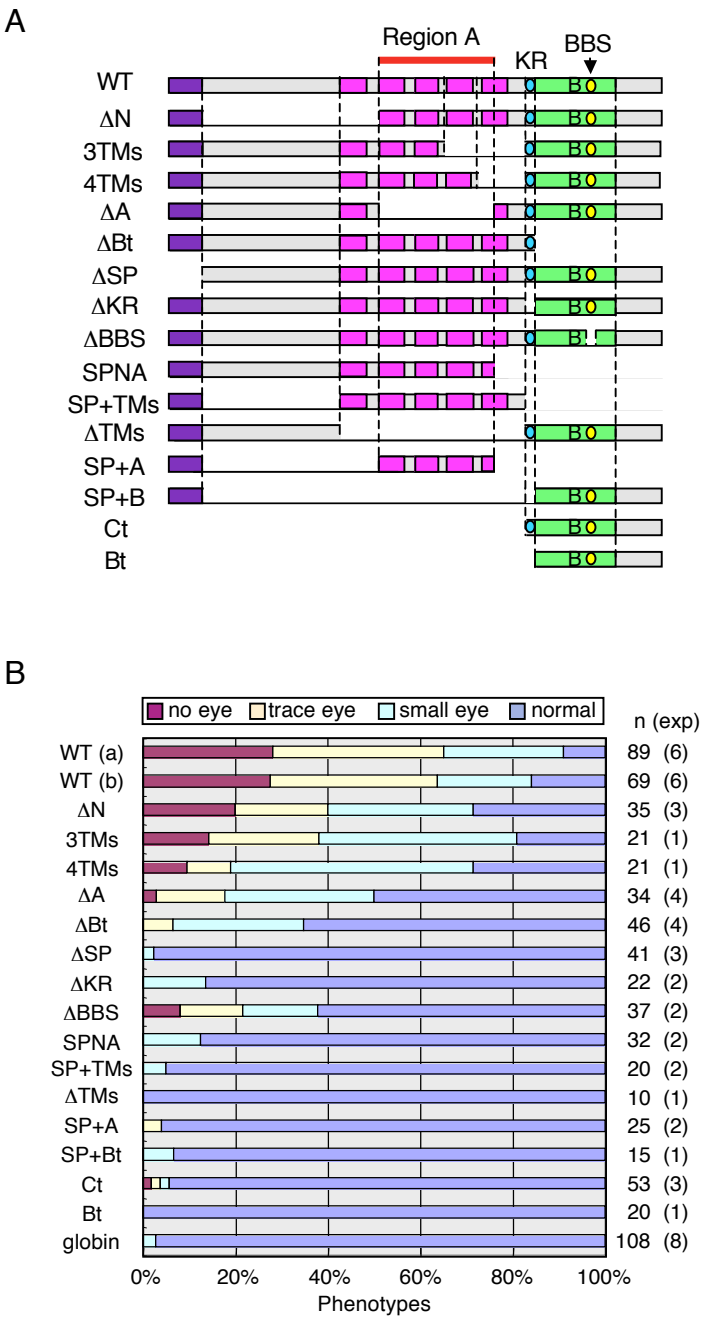
A
Region A
KR
BBS
WT
ΔN
3TMs
4TMs
ΔA
ΔBt
ΔSP
ΔKR
ΔBBS
SPNA
SP+TMs
ΔTMs
SP+A
SP+B
Ct
Bt
B
no eye
trace eye
small eye
normal
n (exp)
WT (a) 89 (6)
WT (b) 69 (6)
ΔN 35 (3)
3TMs 21 (1)
4TMs 21 (1)
ΔA 34 (4)
ΔBt 46 (4)
ΔSP 41 (3)
ΔKR 22 (2)
ΔBBS 37 (2)
SPNA 32 (2)
SP+TMs 20 (2)
ΔTMs 10 (1)
SP+A 25 (2)
SP+Bt 15 (1)
Ct 53 (3)
Bt 20 (1)
globin 108 (8)
0%
20%
40%
60%
80%
100%
Phenotypes

Figure 13

C

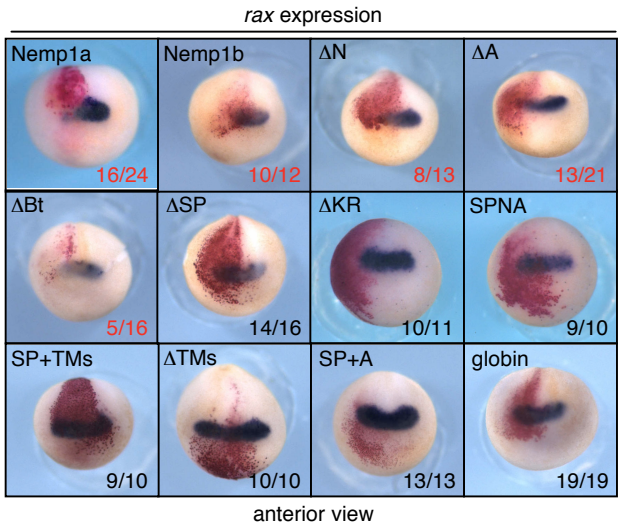

Figure 13 (continued)

Fig. 14. Confocal microscopic analysis of subcellular localization of Nemp1.

Subcellular localization was analyzed by immunostaining as shown in Fig. 1D. C-terminally Myc–tagged deletion constructs of Nemp1 were analyzed by immunostaining (red). Nuclear DNA was stained with SytoxGreen (green). Eye-reducing activities and reduction of *rax* expression of the Nemp1 deletion constructs based on the results in Fig. 5B,C, respectively, were shown in the right of each panel; –, no activity; +, weak activity; ++, moderate activity; +++, strong activity. nd: not determined. Scale bars: 5 μm.

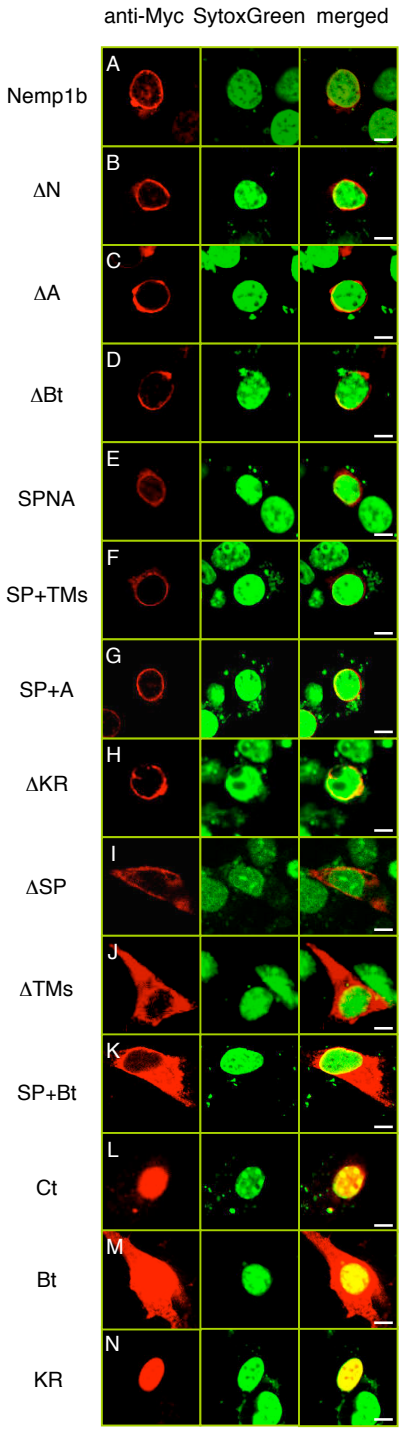
anti-Myc
SytoxGreen
merged
Nemp1b
ΔN
ΔA
ΔBt
SPNA
SP+TMs
SP+A
ΔKR
ΔSP
ΔTMs
SP+Bt
Ct
Bt
KR
A
B
C
D
E
F
G
H
I
J
K
L
M
N

Figure 14

Fig. 15. Relationship between subcellular localization and activity of Nemp1 deletion constructs.

a) nuclear envelope (NE) localization: +, yes; -, no. b) eye defects: +++, more than 80%; ++, more than 60%; +, more than 40%. c) reduction of *rax* expression: +, yes; - no. nd, not determined; NL, nuclear localization.

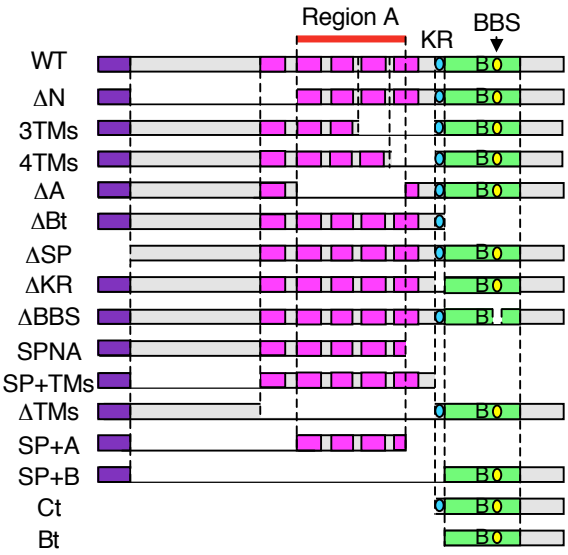

	NE localization[a]	eye defects[b]	*rax* reduction[c]
WT	+	+++	+
ΔN	+	++	+
3TMs	+	++	+
4TMs	+	++	+
ΔA	+	+	+
ΔBt	+	+	+
ΔSP	+/-	-	-
ΔKR	+	-	-
ΔBBS	+	+	nd
SPNA	+	-	-
SP+TMs	+	-	-
ΔTMs	-	-	-
SP+A	+	-	-
SP+B	-	-	-
Ct	- (NL)	-	-
Bt	-	-	nd

Figure 15

Fig. 16. Interactions of BAF with Nemp1.

(A) Alignment of BBS amino acid sequences. BBSs of Nemp1-Ct, MAN1-Ct, Otx2, Crx, and histone H1.1 and a conserved S(R/K)(I/V)XXXX(R/K) motif are shown. Numbers, aa positions.

(B) GST pull-down assay. Purified GST, GST-MAN1-Ct, GST-Bt, and GST-BtΔBBS proteins absorbed onto glutathione-Sepharose were incubated with lysates of *Xenopus* embryos, which had been injected with FLAG-BAF mRNA (500 pg/embryo) or not (control). Bound proteins were separated by SDS-PAGE and immunoblotted with anti-FLAG antibody (upper panel) or CBB staining of GST and GST fusion proteins (lower panel). Comparable amounts of GST and GST fusion proteins were used in the assay (lower panel). Red dots; FLAG-BAF proteins; yellow dots, GST or GST fusions.

(C) Effects of Nemp1 on the intranuclear distribution of BAF in COS7 cells. Expression constructs for Nemp1-HA, ΔBt-HA, or ΔBBS-HA (red) together with FLAG-BAF (green) were transfected.

(D) Effects of Nemp1 on the intranuclear distribution of BAF in *Xenopus* embryos. mRNAs for FLAG-BAF or Nemp1-HA alone (left panels) or both (right panels) were injected into the animal pole region of two cell stage embryos. Injected embryos were immunostained at the gastrula stage (stages 10.5-11). Scale bars: 5 mm.

(E) Requirement of the BBS for the Nemp1 function in eye development. Embryos were injected with MO and mRNA as indicated. Other experimental procedures were the same as in Fig. 11. Phenotypes were analyzed by WISH for *rax* expression.

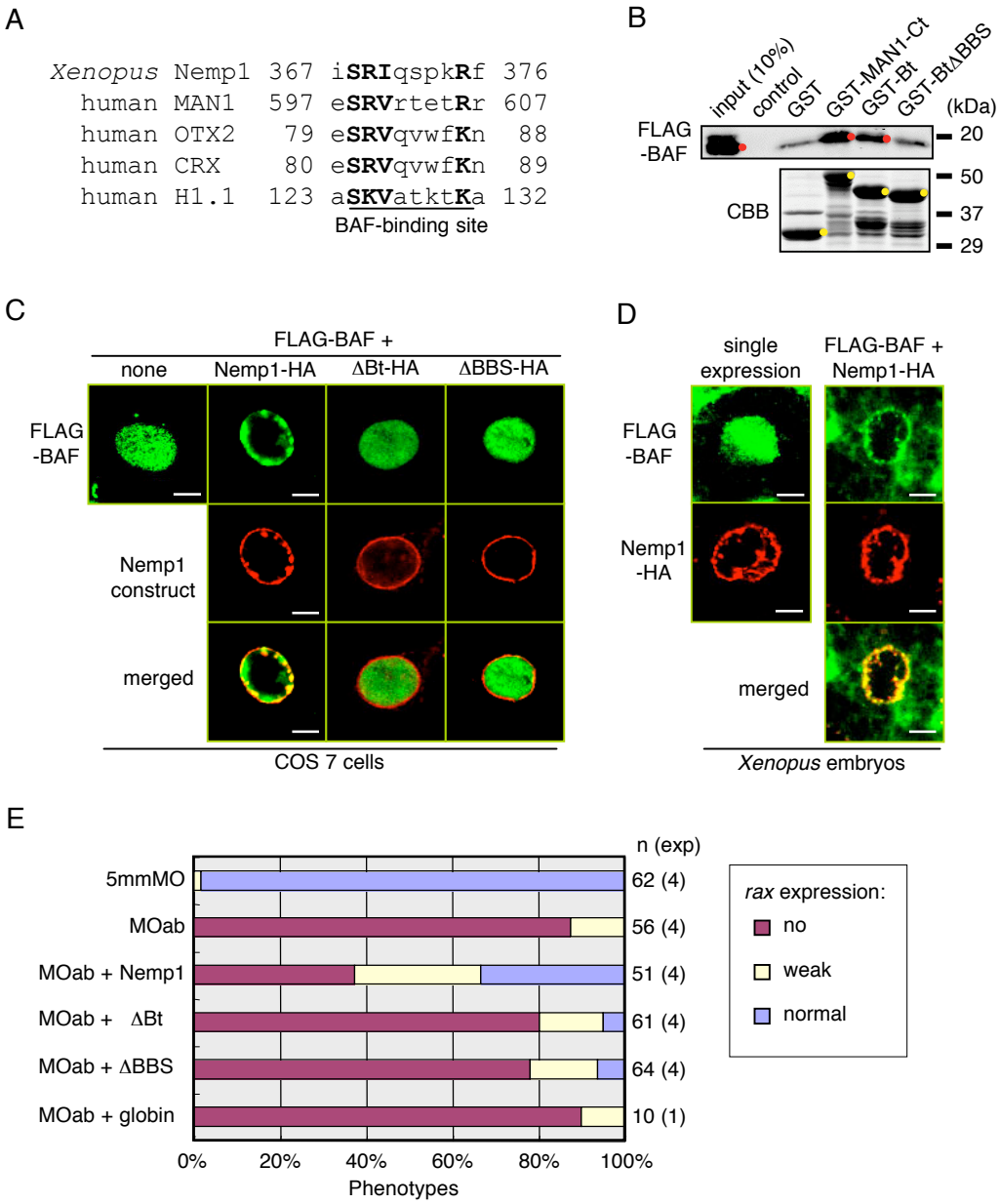
A
Xenopus Nemp1 367 iSRIqspkRf 376
human MAN1 597 eSRVrtetRr 607
human OTX2 79 eSRVqvwfKn 88
human CRX 80 eSRVqvwfKn 89
human H1.1 123 aSKVatktKa 132
BAF-binding site
B
input (10%)
control
GST
GST-MAN1-Ct
GST-Bt
GST-BtΔBBS
(kDa)
FLAG -BAF
CBB
20
50
37
29
C
FLAG-BAF +
none
Nemp1-HA
ΔBt-HA
ΔBBS-HA
FLAG -BAF
Nemp1 construct
merged
COS 7 cells
D
single expression
FLAG-BAF + Nemp1-HA
FLAG -BAF
Nemp1 -HA
merged
Xenopus embryos
E
n (exp)
5mmMO
MOab
MOab + Nemp1
MOab + ΔBt
MOab + ΔBBS
MOab + globin
62 (4)
56 (4)
51 (4)
61 (4)
64 (4)
10 (1)
rax expression:
no
weak
normal
0%
20%
40%
60%
80%
100%
Phenotypes

Figure 16

Fig. 17. A model of Nemp1 localization and function.

A schema of Nemp1 configuration at the INM and interaction with various proteins including BAF are shown. Nemp1 binds to BAF through the BBS at the INM as a complex to activate the Otx2 protein, either directly or in directly, for upregulation of the *rax* gene. BAF also binds to LEM domain and chromatin. KR and Region B possibly interact with some nuclear factors or some transcription factors. Region A may also interact with ONM, INM, or nucleoplasmic proteins. See also the text.

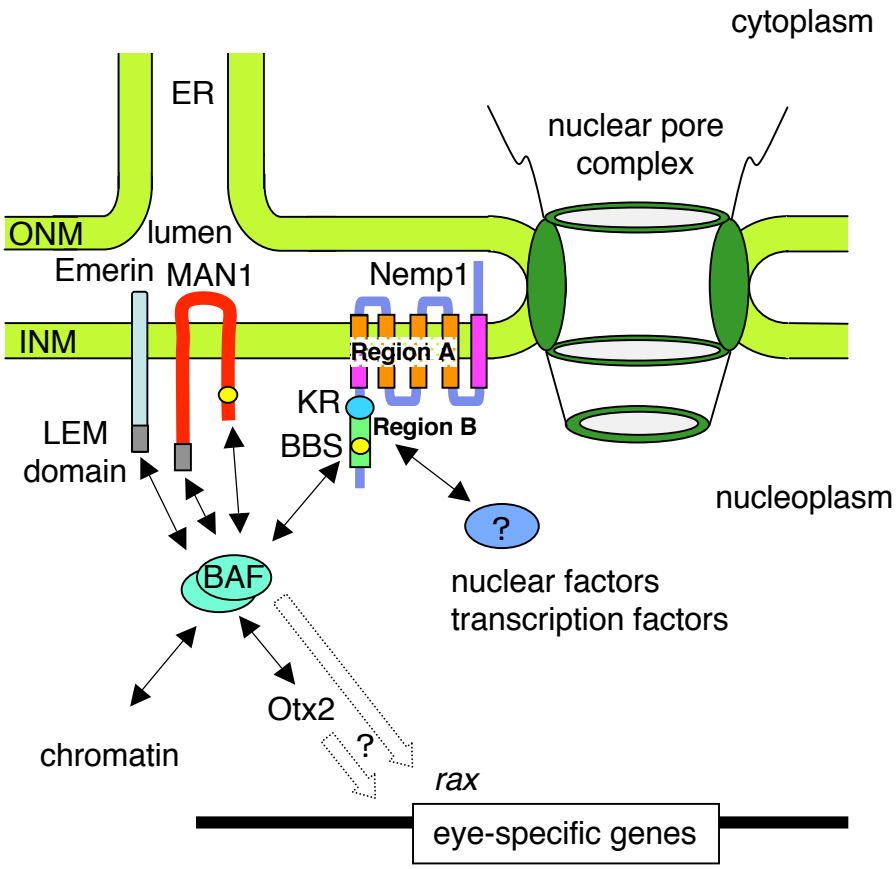
cytoplasm
ER
nuclear pore
complex
ONM
lumen
Emerin
MAN1
Nemp1
INM
Region A
KR
Region B
BBS
LEM
domain
nucleoplasm
?
BAF
nuclear factors
transcription factors
Otx2
chromatin
?
rax
eye-specific genes

Figure 17

Fig. 18. A regulatory cascade for eye field specification and a role of Nemp1 in the anterior neural plate

In the *Xenopus* embryo, a regulatory cascade of eye field transcription factors, Tbx3, Rax, and Pax6 is implicated in eye field specification (Zuber et al., 2003). Note that the expression of *nemp1* overlaps with that of *otx2*. The data in this thesis suggest that Nemp1 functions downstream of Otx2 and upstream of Rax and leads to the possibility that Nemp1 is involved in *rax* expression by Otx2. Expression domains: dark blue, *sox2*; turquoise, *otx2*; light green, *nemp1*; magenta, *tbx3*, *rax*, and *pax6*. See the text.

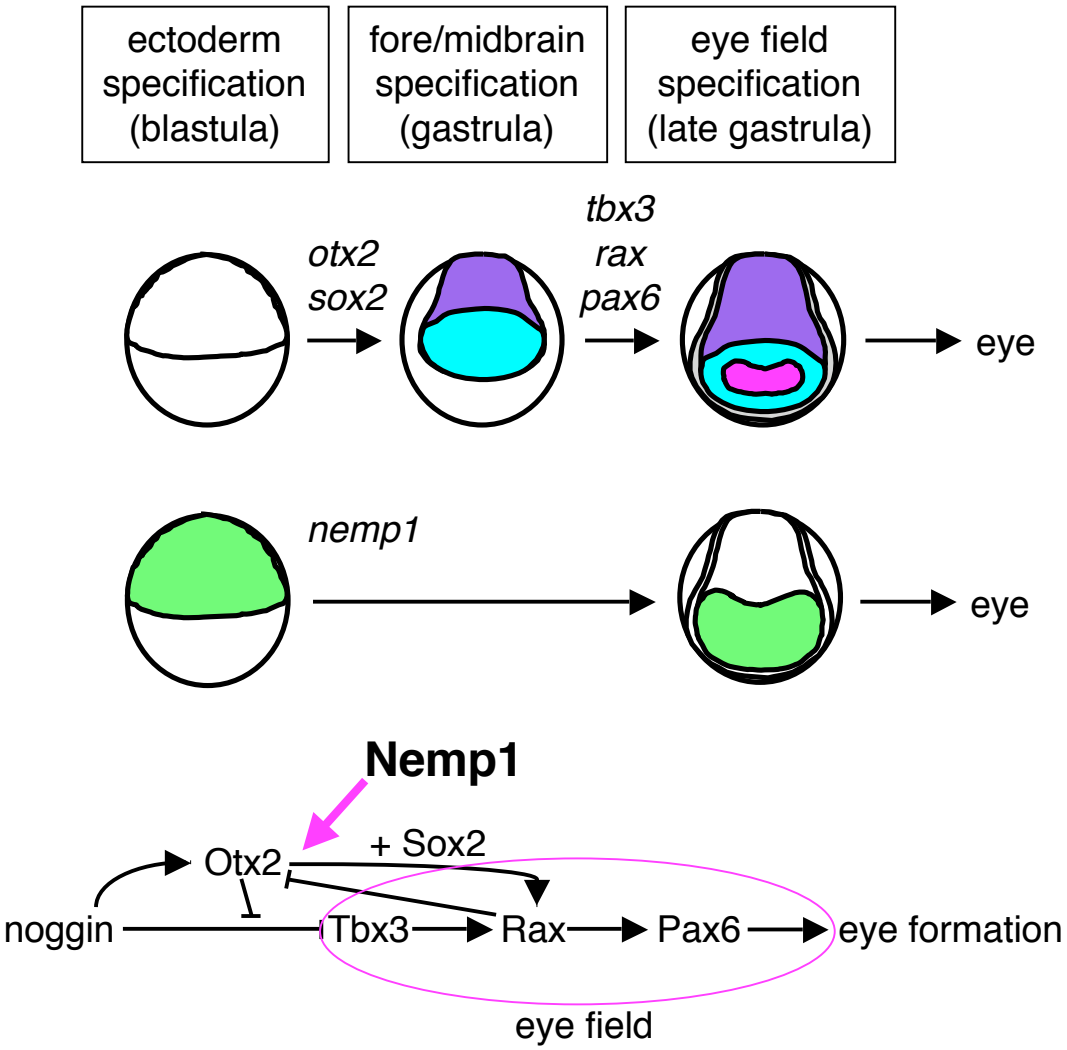
ectoderm specification (blastula)
fore/midbrain specification (gastrula)
eye field specification (late gastrula)
otx2
sox2
tbx3
rax
pax6
eye
nemp1
eye
Nemp1
+ Sox2
Otx2
noggin
Tbx3
Rax
Pax6
eye formation
eye field

Figure 18

Supplementary Figure. The N-terminal tags of HAn-Emerin are not masked in the nucleus in digitonin-treated cells.

COS7 cells were cotransfected with Bt-Myc and HAn-Emerin, and treated with digitonin for 3 min. Other experimental procedures were the same as in Fig. 8. Classification of staining patters is the same as in Fig. 8B except for type X, A', and B', which indicate cytoplasmic staining with no, partial, and complete NE staining, respectively. Types A' and B' are supposedly different from types A and B in Fig. 8B, because NE staining of types A' and B' might indicate the ONM localization of HAn-Emerin with the N-terminus facing the cytoplasm. Note that NE staining of HAn-Emerin was detected mainly in type 2 cells ('accidentally' perforated nuclei), because the ratio of type 2B against total type 2 cells (52%) is much higher than that of type 1B against type 1 cells (8%). This 8% of type 1 cells may indicate the ratio of cells possessing lumenally or cytoplasmically disorientated HA tags. n, total number of transfected cells.

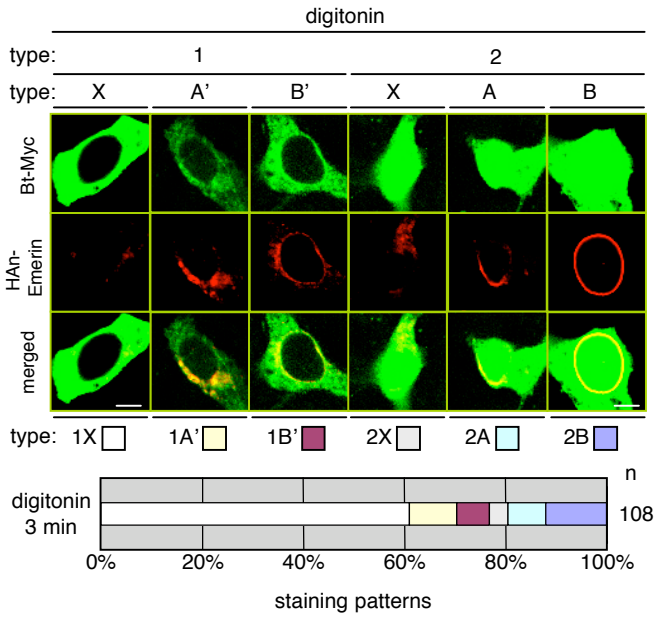

Supplementary figure